AUTOMATED CLASSIFICATION OF RETINAL DISEASES IN STARE DATABASE USING NEURAL NETWORK APPROACH

NAIREEN ZAHEER
Registration Number
00000117735

Supervisor

Dr. Adeeb Shehzaad

Co-Supervisor

Dr. Syed Omer Gilani

DEPARTMENT OF BIOMEDICAL ENGINEERING AND SCIENCES
SCHOOL OF MECHANICAL & MANUFACTURING ENGINEERING
NATIONAL UNIVERSITY OF SCIENCES & TECHNOLOGY
ISLAMABAD, PAKISTAN

AUGUST, 2019

Automated Classification of Retinal diseases in STARE Database Using Neural Network Approach

Author

NAIREEN ZAHEER

Registration Number

00000117735

MS BMS 2015

A thesis submitted in partial fulfilment of the requirements of the degree of MS Biomedical Sciences

Thesis Supervisor

Dr. Adeeb Shehzaad

Thesis Co-Supervisor

Dr. Syed Omer Gilani

Thesis Supervisor's Signature: _____

Thesis Co-Supervisor's Signature: _____

DEPARTMENT OF BIOMEDICAL ENGINEERING AND SCIENCES
SCHOOL OF MECHANICAL & MANUFACTURING ENGINEERING
NATIONAL UNIVERSITY OF SCIENCES AND TECHNOLOGY, ISLAMABAD

AUGUST 2019

Thesis Acceptance Certificate

It is certified that the final copy of MS Thesis written by **Naireen Zaheer** (Registration No. **00000117735**), of SMME (School of Mechanical & Manufacturing Engineering) has been vetted by undersigned, found complete in all respects as per NUST statutes / regulations, is free of plagiarism, errors and mistakes and is accepted as partial fulfilment for award of MS/MPhil Degree. It is further certified that necessary amendments as pointed out by GEC members of the scholar have also been incorporated in this dissertation.

Signature:_____

Supervisor: Dr. Adeeb Shehzaad

Date:_____

Signature:_____

Co-Supervisor: Dr. Syed Omer Gilani

Date:_____

Signature (HOD):_____

Date:_____

Signature (Principal):_____

Date: _____

Declaration

I, Naireen Zaheer, certify that this research work titled ***"Automated Classification of Retinal Diseases in STARE Database Using Neural Network Approach"*** is my own work. The work has not been presented elsewhere for assessment. The material that has been used from other sources has been properly acknowledged / referred.

Signature of Student

NAIREEN ZAHEER

2015-NUST-MS-BMS-0000011773

Plagiarism Certificate

(Turnitin Report)

This thesis has been check for Plagiarism. Turnitin report endorsed by the Supervisor is attached at the end of this report.

_____

Signature of Student

NAIREEN ZAHEER

Registration Number

2015-NUST-MS-BMS-00000117735

_____

Signature of Supervisor

Dr. ADEEB SHEHZAAD

_____

Signature of Co-Supervisor

Dr. SYED OMER GILANI

Copyright Statement

Acknowledgements

I am thankful to Allah Almighty who is most generous and merciful. It is with His guidance and will that I have been able to complete this thesis. Allah has guided me throughout this work at every step and I am thankful to my parents specially my mother for her constant support and her prayers that I have been able to write this thesis and take up every trial into completing my work.

I would like to express my deepest gratitude to my supervisor Dr. Adeeb Shehzaad and my Co- supervisor Dr. Syed Omer Gilani for their valuable and constructive ideas, kind co-operation and inspiration which helped me to complete this research effectively and willingness to give their time generously has been very much appreciated. I also bestow my honor to Sir Zaid Ahsan for his endurance and his vast knowledge which allowed me to believe in my decisions about this research.

I am thankful to Tooba for her advice and ideas that have helped me to complete my thesis. Her support and kind-heartedness has helped me a lot to complete my study. I appreciate the patience, interest, feedbacks and incentive provided by her to achieve my research aims.

I would also like to pay special thanks to my friends Maria Wahid, Shazia Tahir and Armughan Haider for their tremendous support and assistance. Each time I got stuck in something, they came up with the solution. Without their help I wouldn't have been able to complete my thesis. I would also like to thank Anisa and Fatima for being with me as friends. I will like to thank my sister Laraib Zaheer who has helped me to write up this thesis in a smooth manner. Finally, I would like to express my gratitude to all the individuals who have contributed to my study.

Naireen Zaheer

Dedicated to my beloved parents and adored siblings, whose wonderful support and assistance led me to this delightful achievement.

Abstract

The optics of the eye create a visual image of the visual on the retina. Incoming light signal is converted into a neural signal, which in turn is processed by the visual cortex in brain. A healthy retina is crucial for reliable vision. It is vulnerable to organ-specific and systemic diseases as numerous imperative ailments manifest themselves in the retina. Retinal dystrophies and degenerations are often the cause of visual loss and complete blindness in severe cases, hence early diagnosis and appropriate treatment can avert the loss. Various retinal diagnostic techniques performed manually by the ophthalmologist are conventional procedures followed in numerous parts of the world. Since human intervention is highly prone to errors, these strategies don't generally ensure high level of accuracy. Consequently, computerized procedures are significantly crucial for useful applications in the ophthalmology. The purpose of this research was to develop an automated diagnostic system that will be able to identify patients with retinal disorders from images using neural network. This study comprises of four main sections. Data related to retinal pathologies was taken from a publicly available fundus image database. Collected data was then pre-processed by applying exclusion and inclusion criteria on categorized diseases and then visualized. Neural network technique along with three different activation functions (Sigmoid, Gaussian and ArcTan) were used to classify multiple retinal diseases allowing timely detection of such ailments with high accuracy. Sigmoid and Gaussian function gave best performances across all performance metrics. Accuracy calculated for Sigmoid is 0.92, for Gaussian is 0.90 and for ArcTan is 0.46.

Key Words: *Retinal Diseases, Diagnostic Techniques, Neural Network, Accuracy, Sigmoid and Gaussian Functions*

Table of Contents

Thesis Acceptance Certificate iii
Declaration v
Plagiarism Certificate vi
Copyright Statement vii
Acknowledgements viii
Dedication ix
Abstract x
List of Figures xiv
List of Tables xvi
List of Listings xvii
List of Abbreviations xviii
1 Introduction 1
1.1 Human Vision System 1
1.2 Ocular Anatomy & Physiology 1
1.3 Retina – Light Processing Unit 3
1.3.1 Function of Retina 5
1.3.2 Photoreceptors 5
1.4 Retinal Diseases 6
1.4.1 Age Related Macular Degeneration 6
1.4.2 Diabetic Retinopathy (DR) 7
1.4.3 Retinal Vascular Occlusions 8
1.4.4 Hypertensive Retinopathy 12
1.4.5 Retinitis Pigmentosa 15
1.4.6 Coats Disease 15
1.5 Machine Learning (ML) 16
1.5.1 Unsupervised Machine Learning 16
1.5.2 Supervised Machine Learning 17
1.5.3 Neural Network 18
1.6 Publicly Available Databases for Retinal Diseases 20
1.6.1 DIARETDB1- Standard Diabetic Retinopathy Database-Calibration Level 1 20
1.6.2 DIARETDB0- Standard Diabetic Retinopathy Database-Calibration Level 0 21
1.6.3 DRIVE Database 22
1.6.4 DRIONS-DB 22
1.6.5 HRF Image Database 23

1.6.6 STARE Database 23
1.7 Machine Learning Based Classification 24
1.7.1 (1973) 24
1.7.2 (1984) 24
1.7.3 (1998) 24
1.7.4 (1999) 25
1.7.5 (2002) 25
1.7.6 (2007) 25
1.7.7 (2008) 25
1.7.8 (2010) 26
1.7.9 (2012) 26
1.7.10 (2014) 26
1.7.11 (2015) 26
1.7.12 (2016) 27
1.7.13 (2017) 27
1.8 Motivation for Current Study 28
1.9 Objectives of Current Study 28
2 Methodology 29
2.1 Data Acquisition 29
2.1.1 Image Diagnosis 29
2.1.2 Feature Information 29
2.1.3 Disease Information 31
2.2 Data Pre-processing 33
2.2.1 Disease Categorization with Corresponding Image Count 33
2.2.2 Exclusion Criteria for Diseases, Images & Features 33
2.3 Biased Random Sampling 36
2.4 Neural Network Design 37
2.5 Architecture of Neural Network 37
2.5.1 Description of Synapses 37
2.6 Convergence 38
2.6.1 Forward Propagation of Neural network 38
2.6.2 Cost Function and Back Propagation of Neural Network 38
2.6.3 Gradient Descent and Update 39
2.6.4 Iterations 39
2.7 Training Set 39

2.7.1 Activation Functions 39
2.8 Testing Set 40
2.9 Evaluation 41
2.9.1 Accuracy 41
2.9.2 Sensitivity 41
2.9.3 Specificity 41
2.9.4 Precision 41
2.9.5 F1 Score 41
2.10 MATLAB Source Code 42
3 Results 54
3.1 Data Visualization of Training and Testing Data 54
3.1.1 Training Sample Percentages 54
3.2 Iteration Vs Performance of Activation Functions 55
3.2.1 Sigmoid Neural Network 55
1.1.1 Arctan Neural Network 58
1.1.2 Gaussian Neural Network 61
4 Conclusion 64
4.1 Discussions 64
4.2 Conclusions 65
4.3 Recommendations & Future Work 65
References 66

List of Figures

Figure 1- Schematic representation of distinct parts of the Human eye. 2
Figure 2 - Photomicrograph of the retina combined with a diagram of pertinent retinal cells. 4
Figure 3 - Diabetic retinopathy screening phases and diagnostics procedure 8
Figure 4 - Systemic and ocular conditions related to retinal arterial occlusion.....10
Figure 5 – A simple structure of unsupervised machine learning algorithm. 17
Figure 6 – Flow diagram explaining steps of supervised machine learning. 18
Figure 7 – A simple structure of a neuron cell. Main parts include axon, cell body, dendrites and axon terminals. 19
Figure 8 – Architecture of a simple neural network with input, hidden and output layers.....20
Figure 9 – (a) Image010 show signs of major retinal hemorrhage and microaneurysms. **(b)** Image008 has visible hemorrhages and hard exudates in DIARETDB1 Database. 21
Figure 10 – DIARETDB0 images with ground truths. **(Image044) –** include red small dots, hemorrhages hard and soft exudates, neovascularisation. **(Image007) –** contains red small dots, hemorrhages and hard exudates. **(Image013) –** consist of red small dots, hemorrhages and hard exudates.....22
Figure 11 – HRF database images, **(a)** image showing signs of Diabetic Retinopathy, **(b)** image of a healthy retina and **(c)** image of Glaucoma patient. 23
Figure 12 – STARE database images; (IMAGE0001) Background diabetic retinopathy, **(IMAGE0002)** Choroidal neovascularization and arteriosclerotic retinopathy, **(IMAGE0004)** Cilio-retinal artery occlusion or central retinal vein occlusion and **(IMAGE0005)** Central retinal artery and vein occlusion. 24
Figure 13 – Diagnosis for each image present in STARE database. 30
Figure 14 – Thirteen diagnosis codes assigned to diseases by STARE database. 30
Figure 15 – Mapping of 44 manifestation into 39 manifestations. 31
Figure 16 – Diseases represented on x-axis and image count for respective diseases is represented on y-axis. 33
Figure 17 – First exclusion of diseases after two criteria were used. 35
Figure 18 – Second reduction of diseases when both exclusion criteria were applied. Disease 8, 16 and 19 were removed using MATLAB 2017a.....35
Figure 19 – 16 diseases with respective image count. 36
Figure 20 – Architecture of a neural network for retinal disease classification. 37

Figure 21 – This graph is plotted between disease samples and their respective frequency and shows the division of retinal images into training and testing sets, blue color represents total number of positive samples, red color shows all positive training samples while green color shows all positive samples for testing set. 54
Figure 22 – This picture explains the trend observed for normal random sampling (red line) and biased random sampling (green random sampling) for positive samples selected for training of NN and respective diseases. Blue dotted line represents 70 % reference line that depicts 70 %, 30 % split into training and testing set. 55
Figure 23 – Graph is plotted between accuracy on y-axis and 1000 iterations on x-axis (number 10 = 100, 20 = 200, 30 = 300…….100 = 1000 on x-axis). Different color of lines signifies 16 diseases respectively. 56
Figure 24 – F1 score for the designated NN model is plotted between F1 score and number of iterations, highest F1 score can be seen at 500 iterations (number 10 = 100, 20 = 200, 30 = 300…….100 = 1000 on x-axis). 57
Figure 25 – This picture shows the precision trends of 16 diseases across 1000 iterations (number 10 = 100, 20 = 200, 30 = 300…….100 = 1000 on x-axis). 57
Figure 26 – Trends of all diseases for Recall of the system are shown across 1000 iterations (number 10 = 100, 20 = 200, 30 = 300…….100 = 1000 on x-axis)......58
Figure 27 – Specificity was evaluated for 16 selected retinal diseases across 1000 iterations (number 10 = 100, 20 = 200, 30 = 300…….100 = 1000 on x-axis)......58
Figure 28 – This figure illustrates accuracy, precision, specificity, recall and F1 score for Tan^{-1} based NN. All performance measures resulted in overfitting of the data across 1000 iterations (number 10 = 100, 20 = 200, 30 = 300…….100 = 1000 on x-axis)......60
Figure 29 – These graphs represent performance measures for Gaussian NN......63

List of Tables

Table 1: Evaluation and management methods of hypertensive retinopathy......14

Table 2 - STARE database contain a total of 41 diseases, this table provides information of diseases present.....32

Table 3 – This table gives description of final selected 16 diseases.....36

Table 4 – This table describes accuracy, precision, specificity, recall and F1 score evaluated for several iterations......56

Table 5 – Performance table for Arctan neural network......59

Table 6 – Performance table for Gaussian based NN......61

List of Listings

Listing 2.1 MATLAB Code Snippet for Biased Random Sampling 42
Listing 2.2 MATLAB Code Snippet for a Neuron 49
Listing 2.3 MATLAB Code Snippet for NN Design and Training/Testing 50

List of Abbreviations

ANN – Artificial neural network

ARMD–Age related macular degeneration

BRAO – Branch retinal artery occlusion

BRVO – Branch retinal vein occlusion

CNN – Convolutional neural network

CNTF – Ciliary neurotrophic factor

CNV – Choroidal neovascularization

CRAO – Central retinal artery occlusion

CRVO – Central retinal vein occlusion

DIARETDB0– Diabetic Retinopathy Database-Calibration Level 0

DIARETDB1 – Diabetic Retinopathy Database-Calibration Level 1

DME – Diabetic macular edema

DR – Diabetic retinopathy

DRIONS-DB – Digital Retinal Images for Optic Nerve Segmentation Database

DRIVE – Digital Retinal Images for Vessel Extraction

FN – False negative

FOV – Field of view

FP – False positive

GT – Ground truth

HIV – Human immunodeficiency virus

HRF – High resolution fundus

IL-6 – Interleukin 6

ML – Machine learning

MLP –Multilayer perceptron

NN – Neural network

OCT – Optical coherence tomography

OD – Optic disc

PCA – Principal component analysis

PDR – Proliferative diabetic retinopathy

PNN – Probabilistic neural network

RAO – Retinal artery occlusion

RCI – Relative classifier information

RD – Retinal detachment

RdCVF – Rod derived cone viability factor

ReLU – Rectified linear unit

ROC – Receiver operating curve

RP – Retinitis pigmentosa

RPE-Retinal pigment epithelium

RVO – Retinal vein occlusion

STARE – Structured analysis of retina

SVM – Support vector machines

TN – True negative

TP – True positive

VEGF – Vascular endothelial growth factor

1 Introduction

This section mainly explains the functional and anatomical characteristics of the retinal diseases and advanced automated image analysis methods. Firstly, a brief outline of the Human eye and the retina is elucidated. Secondly, different retinal diseases and how these abnormalities are related through certain features is discussed. A summary of the retinal imaging techniques and publicly available image databases is given. Then, a description of the prevailing modern techniques for the computer aided detection and classification of retinal ailments is narrated.

1.1 Human Vision System

Among five senses of the human body, sense of vision is the most used. Eyes provide spatial information about the surrounding world. The human eyes and brain work together to analyze the incoming visual information, this procedure is ordinarily alluded to as visual processing. The human eye is frequently equated to a digital camera, both have lenses to centers the approaching light. Unravelling the complication of altering light into ideas of visual perception of the world is a complex task.

1.2 Ocular Anatomy & Physiology

One of the incredibly astounding and intricate sensory system of the human body is the eye. The eye is roughly spherical in shape, sometimes called as spherical globe, with a thickness of nearly 24 mm antero-posteriorly (Bjorn et al., 2009). It can mainly be divided into three layers as;

- Outer layer - includes cornea, lamina cribrosa and sclera,
- Middle layer - also referred as vascular layer of the eye, it is made of iris, choroid and ciliary body,
- Inner layer – has an intricate layered structure called Retina including retinal pigment epithelium, photoreceptors and neurons.

A graphic illustration of the anatomy of eye is represented in Figure 1. There are three sections of the eye i.e. anterior, posterior and vitreous chamber. The *anterior part* of the eye comprises of the cornea, iris, pupil, and the lens. *Posterior chamber* is a triangle shaped area

located in between iris, lens and the ciliary body. Lastly, there is a cavity present behind the lens and zonule called as *vitreous chamber* (Bjorn et al., 2009).

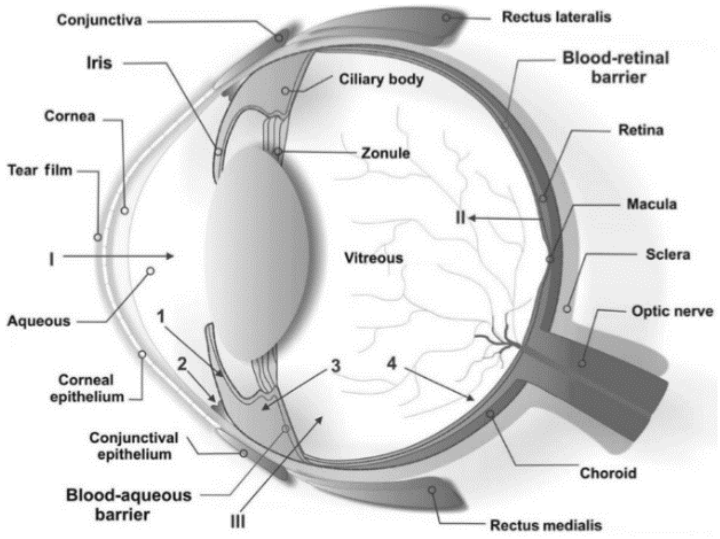

Figure 1- Schematic representation of distinct parts of the Human eye.

Another part of the anatomy of the eye is the intraocular fluids, three types of fluids are there:

- Aqueous humour – a clear watery fluid with minimal protein content.
- Vitreous humour – is a translucent gel containing a three-dimensional meshwork of collagen fibers. It fills the gap among the posterior surface of the lens, ciliary body and retina.
- Blood – promotes the preservation of intraocular pressure (Sliney & Wolbarsht, 1980).

A huge segment of the blood inside the eye is in the choroid. The choroidal blood stream connotes the significant blood stream per unit tissue in the body. The dimension of desaturation of efferent choroidal blood is nearly little and assigns that the choroidal vasculature has works past retinal nourishment. It may be that the choroid helps as a heat exchanger for the retina, which captivates energy as light strike with the retinal pigment epithelium.

The outermost layer of the eyeball is an opaque white colored membrane called the sclera. There is a minor protuberance in the sclera which is the anterior of the eye. The cornea is translucent, avascular and compactly innervated tissue of the body. It acts similar to a camera lens and primarily centers the incoming light signal. The iris is a muscle that contracts and expands, hence forming a round opening which varies in size and controls the light going into

the eye by adjusting the size of the pupil (Willoughby et al., 2010). The lens is situated right at the rear of the pupil and further focuses light signal. It is made up of closely packed epithelium layer that covers a cluster of fibers which refines light from the cornea. Light centered by the cornea and lens at that point stretch to the retina. The retina in turn converts the perceived optical pictures into electronic signals that are transferred to brain through optic nerve (Zhu, Zhang, & Del Rio-Tsonis, 2012).

1.3 Retina – Light Processing Unit

Retina is 0.5 mm thick, multilayered coat of neural tissue closely attached to a single layer of pigmented epithelial cells. It is a sensory organ and a light processing center of the eye. Incoming light signal is changed into neural signal which in turn is processed by the visual cortex in brain. It is composed of a fine layer of cells that borders the interior side of the eye.

Mainly specialized neural cells and light sensitive cells combine to form the retina. These neural cells are unusually comparable to those of the brain, supporting the common statement that the visual structure is an extension of the central nervous system (Zhu et al., 2012). Sensory retina is partitioned into nine evident layers expanded from the vitreous to choroid as depicted in figure 2 (Gupta, Herzlich, Sauer, & Chan, 2016).

The layers of the retina in figure 2 are acknowledged along the left column of the image. The corresponding cell types are labeled on the right-hand side of the image in figure 2. The layers vary from the internal limiting membrane to the retinal pigment epithelial (RPE) at the outer end. The basic descriptions of each of the 10 layers of the retina are started below the photomicrograph of the retina of figure 2.

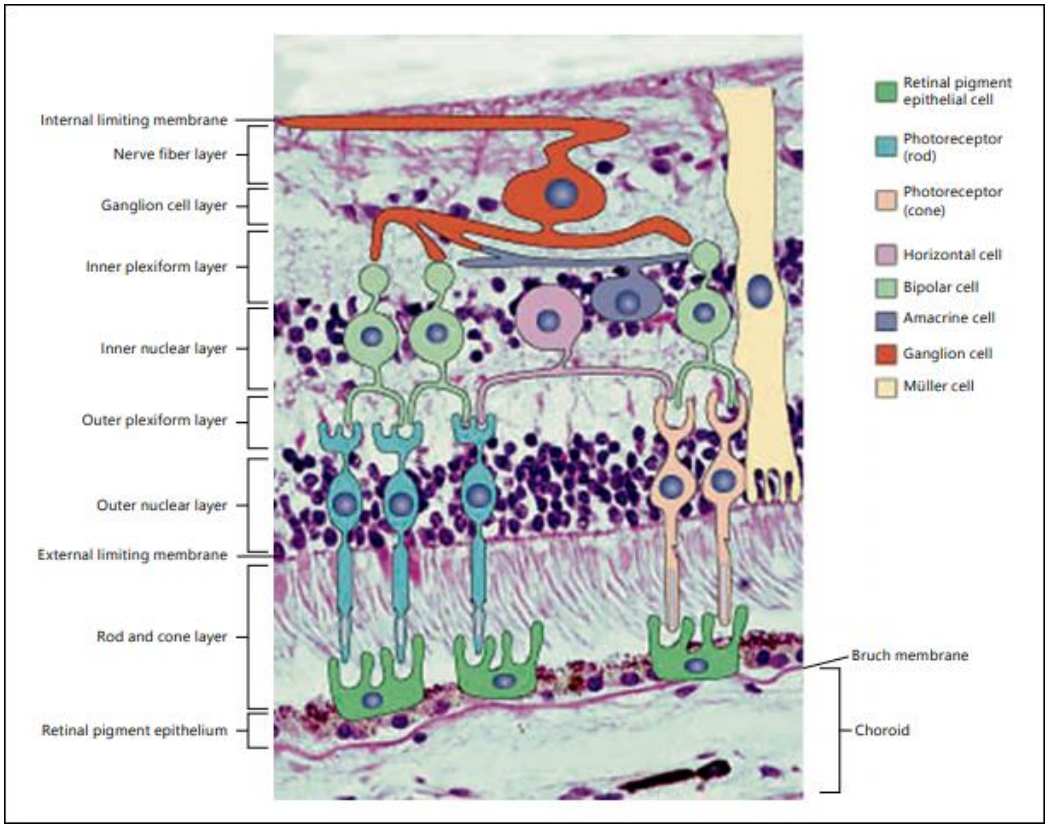

Figure 2 - Photomicrograph of the retina combined with a diagram of pertinent retinal cells.

(1) Internal limiting membrane is made up of vitreal and retinal elements by the enlargement and flattening of Müller cells.

(2) Nerve fiber layer has the axons of the ganglion cells and are minimalistically pressed together and converge into the optic disc. These axons travel to the optic nerve head inside this layer. Nerve fiber layer is denser around optic disc as a result of conjunction of ganglionic axons on the disc.

(3) Ganglion cell layer*:* Axons of ganglion cells are located in the nerve fiber layer while the cell bodies of these cells combine to form this layer.

(4) Inner plexiform layer: Ganglion cell dendrites spread into the inner plexiform layer where they create synapses with other interlocked cells, whose cell bodies are found in the next layer.

(5) Inner nuclear layer: Ganglion cell dendrites form a connection through synaptic interaction among other intertwined cells whose cell bodies lies inside inner nuclear layer, hence creating this layer.

(6) Outer plexiform layer: comprise synaptic networks of photoreceptor cells.

(7) Outer nuclear layer: Cell bodies of the photoreceptors are situated in this layer.

(8) External limiting membrane is not actually a sheath, nonetheless relatively includes tightly packed joints amongst photoreceptors and supporting cells.

(9) Receptor layer: The photoreceptors exist in the receptor layer. Naturally, photoreceptors are of two kinds i.e. *rods and cones*. (Bjorn et al., 2009; Hildebrand & Fielder, 2011).

(10) Retinal pigment epithelial (RPE): A single sheet of cuboidal cells called retinal pigment epithelium is present beneath the photoreceptors consisting of melanosomes. From these melanosomes cells usually derive their pigmented color. The RPE cells functions to nurture the outer neurosensory retina, responsible for facilitated diffusion of nutrients and eradicates the waste photoreceptor parts (Gupta et al., 2016).

1.3.1 Function of Retina

The humungous structure of the human eye is regularly contrasted to a camera. Light rays pass through various parts of the eye and are altered into electrical impulses by the retina. Primarily, cornea and aqueous humour focuses light rays. Lens furthers focuses the light signal with the help of a muscle called *Zonula* by controlling the position and shape of the lens. The iris regulates the extent of light signal coming in the eye by changing the size of the pupil. Incoming light signals are then focused onto the retina which transforms into electrical impulses that are carried to brain across optic nerve for further processing in the visual cortex (Sebastian, 2010).

1.3.2 Photoreceptors

Photoreceptors are sensors of retinal system and converts the photons into a nerve signals (process termed photo transduction). These impulses are converted into images while moving along optic nerve. The outer segment membranes of photoreceptors contain pigments. Photoreceptors are of two kinds:

- Rods
- Cones

Rod cells are oblivious to color; they are largely present at the edge of retina, usually used for night vision (scotopic) and can spot movement. Highly precise cells called cones are mainly present in macula and are responsible for day vision (photopic). They are able to detect colors (Willoughby et al., 2010; Wyszecki & Stiles, 1982).

1.4 Retinal Diseases

A healthy retina is crucial for improved vision. Due to modern living styles of human beings, various parts of the retina are affected and cause vision impairments. The retina is susceptible to organ-explicit and systemic sicknesses as numerous imperative ailments show themselves in the retina and initiate either in the eye, the brain or the cardiovascular system (Abramoff, Garvin, & Sonka, 2010). Retinal diseases continue to be a key contributor to reduced sight exclusively in the elderly populace. Retinal dystrophies and degenerations are often the cause of visual loss and complete blindness in severe cases (Banerjee, 2006; Kannabiran & Mariappan, 2018). The limit of retinal tissue to react to such injuries depends to a great extent on the particular cells and tissue involved, and in addition the type, extent and seriousness of the damage (Gupta et al., 2016). Some of the most important diseases are described briefly.

1.4.1 Age Related Macular Degeneration

Age-related macular degeneration (ARMD) is amongst the most common retinal disorder whose occurrence is more prominent in elderly populace. It is of two types that have different manifestations, dry AMD and wet AMD.

- **Dry AMD:** also called as atrophic macular degeneration causes gradual damage of visual acuity. Almost 90% of cases are for dry AMD (Visser, 2006). It is categorized by drusen (yellow white spots), extracellular residues, that agglomerate underneath the RPE in Bruch's membrane, and damaged photoreceptors and RPE (Gupta et al., 2016; Jager, Mieler, & Miller, 2008).
- **Wet AMD:** is also referred to as exudative AMD, significant feature of this category is choroidal neovascularization (CNV). It is far less common than the nonexudative AMD as it accounts for about 10 % cases as compared to the other type (Visser, 2006). A choroidal vascular assembly grows into the macula causing vascular penetrability. Sub retinal or intra retinal fluid is collected in the vicinity which ultimately leads to visual impairment to a threatening level. Hemorrhages also occurs in CNV damaging the overlying photoreceptors (Coleman, Chan, Ferris, & Chew, 2008; Jager et al., 2008).

1.4.1.1 Diagnostic Techniques

Fundus photography, visual acuity examination, dilated eye test and fundoscopy can be used for diagnosis of all types of ARMD. Progression of dry AMD can be reduced using some dietary supplements (Abramoff et al., 2010), however, for wet form of AMD, intravitreal

injections of anti-VEGF drug such as ranibizumab are used for treatment (Lim, Mitchell, Seddon, Holz, & Wong, 2012; SPAIDE et al., 2006).

1.4.2 Diabetic Retinopathy (DR)

Individuals with diabetes have greater possibility of developing diabetic retinopathy. Minor changes in vasculature caused by the high blood sugar level may damage the retinal blood vessels and bring about extreme vision damage or blindness. Diabetic retinopathy is an impediment of diabetes mellitus and is one of the most common bases of blindness. Elevated blood sugar level causes the degeneration of blood vessels in different ways like,

- Insufficient blood supply to some parts of the human body causes formation of new blood vessels which possibly will bleed afterwards or instigate retinal detachment, a disorder termed as **proliferative diabetic retinopathy (PDR).**
- Fluid from the blood vessels may leak into the surrounding area sometimes causing the breakage of blood-retinal barrier and deteriorating the light sensitive photoreceptors, referred to as **diabetic macular edema (DME)** (Abramoff et al., 2010).

1.4.2.1 DR Screening

Fundus photography, clinical eye check-up, OCT, direct ophthalmoscopy and fluorescein angiography are some diagnosis techniques used for DR screening (Oetting Thomas & Jesse Vislisel, 2010). DR management and evaluation is described in figure 3 (T. Kauppi et al., 2007).

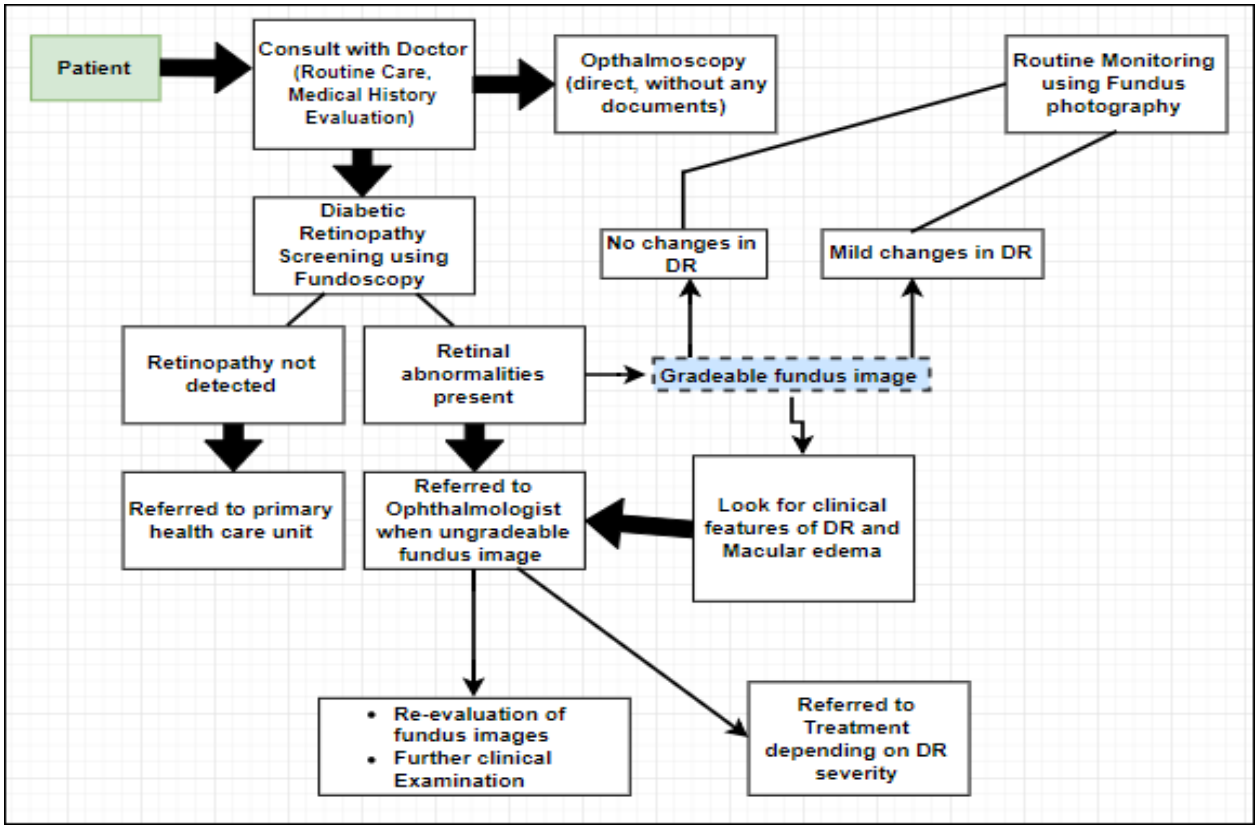

Figure 3 - Diabetic retinopathy screening phases and diagnostics procedure

1.4.3 Retinal Vascular Occlusions

One of the conventional reasons of visual impairment is occlusive diseases of the retina that may result mainly because of systemic diseases (e.g. cardiovascular disease). The diagnosis primarily rest on the location, level, period and extent of retinal obstruction (Mirshahi, Feltgen, Hansen, & Hattenbach, 2008). Clinical manifestation of retinal vascular occlusion includes gradual, painless vision loss. Anatomical area where blockage is present determines the type of occlusion (Bradvica, Benašić, & Vinković, 2012).

1.4.3.1 Retinal Artery Occlusion (RAO) -

Retinal artery occlusion is defined as obstruction of the retinal artery that give nutrients and oxygen to the nerve cells in the retina. The deficiency of oxygen transfer to the retina may cause extreme painless vision loss. Blood supply to the brain and retina is identical as retina is the part of nervous system as well as carotid artery (Pei & Rhodin, 1970). RAO is frequently linked with perilous cerebrovascular and cardiovascular disease.

It is categorized into two forms, central retinal artery occlusion (CRAO) and branch retinal artery occlusion (BRAO).

1.4.3.1.1 Central Retinal Artery Occlusion (CRAO)

It is an ophthalmic crisis and the visual equivalent of cerebral stroke as both have a common pathology in terms of certain hazardous aspects such as diabetes mellitus, hypertension and hyperlipidemia (Hayreh, Zimmerman, Kimura, & Sanon, 2004). The level of blindness depends on the nature of the obstruction. Vision loss or blurry visual acuity is central and condensed in this type (S. Rumelt & Brown, 2004).

Occlusion of the central retinal artery result in the inner retinal layer edema which in turn cause ischemic necrosis and the retina turn out to be blurred and yellow-white color emerges (KEARNS & HOLLENHORST, 1963). Retinal artery obstruction may arise caused by

- embolism,
- vaso-destruction including atherosclerotic plaques, giant-cell arteritis and some forms of vasculitis),
- vascular compression with neoplasm,
- angio-spasm (Bradvica et al., 2012; Hayreh, Podhajsky, & Zimmerman, 2011; Körner-Stiefbold, 2001).

1.4.3.1.2 Branch Retinal Artery Occlusion (BRAO)

Segmental visual damage occurs if a small artery or branch retinal arterioles are obstructed and the affected area may involve a segment of the peripheral visual field space (S. Rumelt & Brown, 2004). Retinal edema is the distinctive feature of this type of occlusion affecting more distal arteries of the retina when the affected artery is blocked by an embolus retinal whitening appears in the affected vessel (Hayreh et al., 2011; Noma, Funatsu, Mimura, & Hori, 2008).

BRAO may be permanent or transient (if blockage clears and blood supply is restored) wholly based on the type of occlusion in the retinal artery (Bradvica et al., 2012).

1.4.3.1.3 Treatment of Retinal Arterial Occlusions (RAO)

In case of RAO, it is crucial to know beforehand the source of occlusion in retinal arteries to better diagnose and treat the disease (Hayreh et al., 2004; Jain & Juang, 2009). Certain systemic and some other ophthalmic conditions also helps in initiation or progression of RAO some of which are explained in figure 3. Certain imaging modalities are available to diagnose patients with arterial occlusions including

- electroretinography,
- optical coherence tomography (OCT),
- fluorescein angiography,
- fundoscopy and
- visual field testing.

Vasodilation, decreasing intraocular pressure, hyperventilation, heparin or antiplatelet treatment are some methods used as conservative type of treatment on the other hand, invasive treatment modalities are also being used (Bradvica et al., 2012).

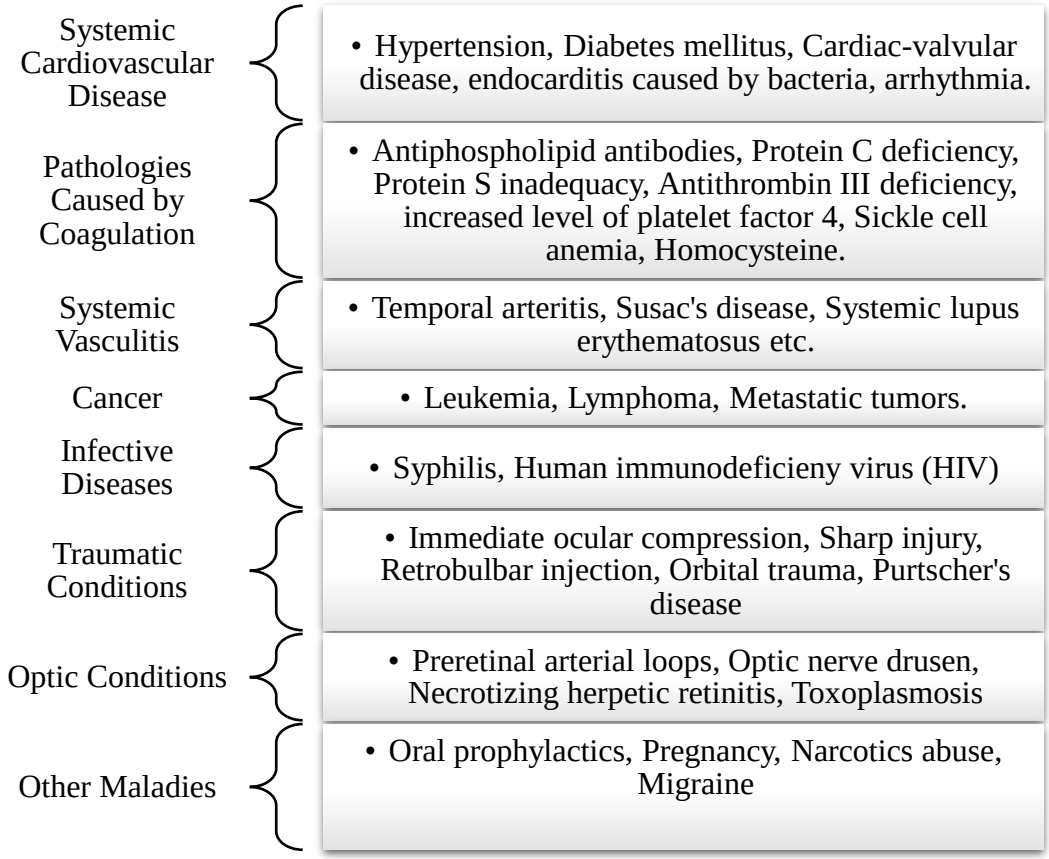

Figure 4 - Systemic and ocular conditions related to retinal arterial occlusion

1.4.3.2 Retinal Vein Occlusions (RVO)

Another highly usual source of severe visual impairment is retinal vein obstructive disorders that are associated with numerous risk factors and systemic illnesses including hypertension, diabetes mellitus, and vasculitis (Laouri, Chen, Looman, & Gallagher, 2011; Marcucci, Sofi,

Grifoni, Sodi, & Prisco, 2011). Depending on the type and area of occlusion, RVO can be categorized into two classes (1) Branch retinal vein occlusion (BRVO) and (2) Central retinal vein occlusion (CRVO). BRVO arises more frequently than the other type and the site where BRVO arises is often the junction of a vein and artery. While CRVO is less common in occurrence and usually arises from a thrombus residing in the central vein of the retina at the point of lamina cribrosa (Esmaili & Boyer, 2018).

1.4.3.2.1 Branch Retinal Vein Occlusion (BRVO)

Branch retinal vein occlusion take place in distal vein branches of retina and is further divided into major BRVO (when one of the main branch veins of retina is blocked) and minor BRVO (when small veins near the macula are obstructed; also called as macular BRVO). Compression of adjacent vein at arterial vein junction is the key manifestation of BRVO that cause turbulent flow in the veins, degeneration of retinal vessels and irregular levels of hematological factors (Marcucci et al., 2011; Rehak & Rehak, 2008).

1.4.3.2.2 Management of BRVO

Macular edema is one of the prevailing signs of BRVO and develops because of irregular expression of vascular endothelial growth factor (VEGF) and interleukin-6 (IL-6) when the retinal veins are occluded. Distinctive clinical symptoms of BRVO include dot and blot hemorrhage, hard and soft exudates, edema and vasodilation. Fluorescein angiography, optical coherence tomography (OCT), fundoscopy and slit lamp are utilized to examine patients with BRVO (Rehak & Rehak, 2008). Grid laser photocoagulation is one of the medication methods for macular edema in BRVO. Certain other therapies are available for this disease including

- Injections of anti-VEGF drugs,
- Anti-aggregative remedy and fibrinolysis,
- Isovolaemic hemodilution,
- Intravitreal corticosteroids and periocular use of steroids (Esmaili & Boyer, 2018).

1.4.3.2.3 Central Retinal Vein Occlusion (CRVO)

The progression of central retinal vein occlusions is a complex multistep process. Changes in the central artery wall because of Atherosclerosis leads to the amplified intraocular pressure (IOP) and compression of central venous wall that results in thrombus formation and hence, vein occlusion (Mirshahi et al., 2008). Ischemia and hypoxia are another contributing factor in severity of the disease. Intra retinal hemorrhages, swelling of the optic disc (OD) and

appearance of cotton wool spots rigorously affects the visual acuity. CRVO is divided into two subtypes

a) Ischemic CRVO – Elevated capillary pressure in vascular network of retina results in sites where there is no blood flow and sites where blood is retained causing hemorrhage, neovascularization due to high levels of VEGF and referred to as ischemic CRVO.
b) Non- ischemic CRVO – it is often observed if there are no non-perfusion capillary areas in the vascular system of retina (Boyd et al., 2002; Noma et al., 2008; Pe'er et al., 1998).

1.4.3.2.4 Management of CRVO

Most crucial factor in diagnosing central retinal vein occlusion is to differentiate between its types i.e. ischemic and non-ischemic. Normally fundus photographs reveal the signs of both kind of CRVO that depends on how much area of fundus is affected by hemorrhages while fluorescein angiography confirms the extent of ischemia and macular edema in some cases. To further check the presence of edema in macula, optical coherence tomography (OCT) is useful as it is a non-invasive method (Mirshahi et al., 2008; Patel, Nguyen, & Lu, 2016). A variety of treatments exist for CRVO, some of which are:

- Decreasing venous compression using surgical operations such as vitrectomy, optic nerve sheet decompression and neurotomy.
- Anastomosis of chorioretinal veins.
- Anticoagulant remedy.
- Biodegradable implants (Golan, Fisher, & Lowenstein, 2011).
- Injecting drugs into the vitreous area of the eye.
- Diverse types of photocoagulation such as thermic laser coagulation, venous dissection etc (Mirshahi et al., 2008; Stahl, Agostini, Hansen, & Feltgen, 2007).

1.4.4 Hypertensive Retinopathy

Hypertension occurs due to elevated rise in blood pressure. It is a leading cause of certain pathophysiological disorders such as metabolic disturbances, oxidative stress, hypertrophy

inflammation etc. Certain environmental and genetic risk factors lead to hypertension for instance (Delacroix, Chokka, & Worthley, 2014; Natalie Schellack, 2015),

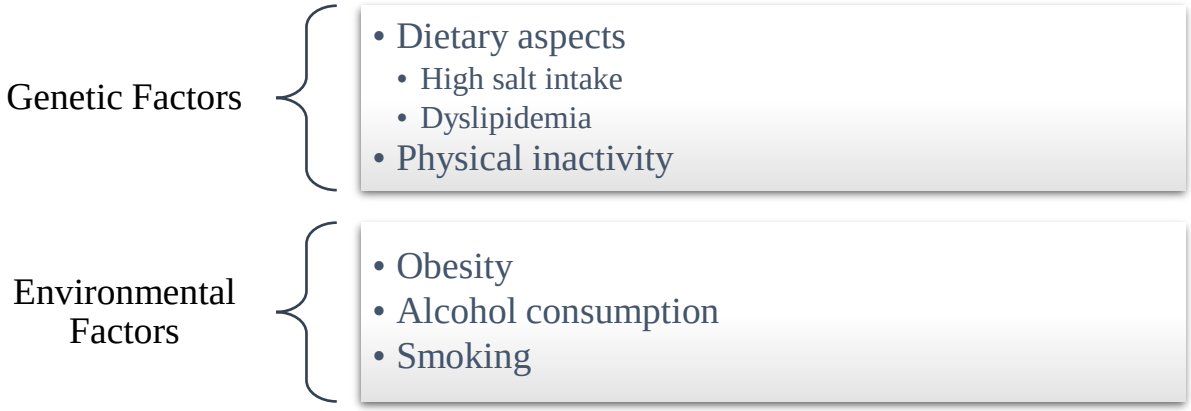

Certain important human body systems are involved in incidence of systemic hypertension including cardiovascular, renal, ocular, endothelial and sympathetic nervous system leading to vascular constrictions, macro aneurysm etc. Retinal vasculature also develops abnormal changes usually termed as hypertensive retinopathy (Ma & Yu, 2016).

Liebreich first coined hypertensive retinopathy in 1859. According to Liebreich, hypertensive retinopathy is the result of end stage organ damage due to elevated arterial blood pressure and other specific risk factors (Chatterjee, Chattopadhya, Hope-Ross, Lip, & Chattopadhya, 2002).

1.4.4.1 Clinical Manifestations & Management of Hypertensive Retinopathy

Various pathophysiological changes cause acute, chronic, severe or accelerated hypertensive retinopathy. Clinical features of this disease are elevated blood pressure, thinning of the arterioles because of vasospasm (Garner & Ashton, 1979), opacification of retinal artery walls also called as copper/silver wiring of retina, distinct types of hemorrhages, hard exudate formation due to dyslipidemia etc., micro aneurysm, nicking of artery and veins of retina, emboli, OD swelling, cotton wool spots (Chatterjee et al., 2002; Erden, Mefkure Ozkaya, Banu Denizeri, & Karabacak, 2016; Grosso, Veglio, Porta, Grignolo, & Wong, 2005).

Hypertensive retinopathy generally classified as mild, moderate and accelerated retinopathy and related to some important systemic diseases, diagnosis of this disorder and some treatment modalities are described in the Table 1 (Aronow, 2012; Chen, Kuo, & Kao, 2003; Natalie Schellack, 2015; Wong & McIntosh, 2005).

Table 1: Evaluation and management methods of hypertensive retinopathy.

HYPERTENSIVE RETINOPATHY TYPE	ASSOCIATED SYSTEMIC DISEASES	DIAGNOSTIC TECHNIQUES	TREATMENT METHODS
Mild/Minor	▪ Stroke ▪ Coronary heart disease ▪ Mortality of cardiovascular system	▪ Medical history ▪ Echocardiogram ▪ Fundoscopy ▪ Blood pressure check and balance ▪ Routine care (examining environmental risk factors such as smoking, salt intake, obesity etc.) ▪ Lipid profiling	▪ Lifestyle alteration ▪ Routine Analysis ▪ Initial laboratory tests
Moderate	▪ Congestive heart failure ▪ Stroke ▪ Renal malfunction	▪ Inspecting cholesterol level ▪ Electrocardiogram ▪ Fundus photography ▪ Urine analysis ▪ Renin/Aldosterone level	▪ Reduction of factors causing high cholesterol level (reduction therapy)
Accelerated	▪ Kidney failure ▪ Mortality	▪ Hourly blood pressure control ▪ Fundus photography ▪ X- ray	▪ Anti hypertensive drug therapy ▪ Ocular adjuvant treatments targeting VEGF

1.4.5 Retinitis Pigmentosa

Retinitis pigmentosa (RP) is a cluster of genetically transferred diseases of the posterior part of the eye distinguished by deterioration in central periphery of fundus, atrophy and cause loss of photoreceptors and visual loss lead by retinal pigment epithelium (Konieczka, Flammer, Todorova, Meyer, & Flammer, 2012). Rod-cone dystrophy is the normal type of RP, starting with night blindness, loss of marginal visual field. Common symptoms for RP are Night blindness, atrophy of the RPE, Photophobia, Ring shape scotoma, Tunnel vision, many degrees of atrophy etc. It is inherited by autosomal-recessive, autosomal-dominant or in X- linked fashion (Hamel, 2006).

1.4.5.1 Management of RP

Optical coherence tomography (OCT), Fluorescein angiography and visual field testing are the diagnostic techniques used for detection of signs and symptoms of Retinitis pigmentosa (Shintani, Shechtman, & Gurwood, 2009). Certain treatment modalities are available worldwide for retinitis pigmentosa some of which are:

- Gene therapy
    - Viral-mediated gene supplementation therapy
    - Adeno-associated virus delivery
    - Choroideremia
- Stem cell transplantation
- Electronic retina implant
- Pharmacological therapy
    - Ciliary neurotrophic factor (CNTF)
    - Rod derived cone viability factor (RdCVF) (Lin, Tsai, & Tsang, 2015)

1.4.6 Coats Disease

An olfactory, idiopathic disease called “Coats” caused by shortcoming in the growth of retinal vascular system generated by internal bleeding, retinal telangiectasis, intra and sub-retinal exudation. George Coats in 1908, first described coats as a unilateral, advancing condition affecting males during childhood between 8 to 16 years.

Symptoms include loss of pericytes and endothelial cells, dilated telangiectasis, degeneration of abnormal pericytes results in aneurysms, closing of vessels (Ghorbanian, Jaulim, & Chatziralli, 2012).

1.4.6.1 Diagnosis:

- Ophthalmic B-scan ultrasonography
- Fluorescein angiography
- Optical coherence tomography
- Computed tomography
- Magnetic imaging resonance

1.4.6.2 Treatment Methods:

- Cryotherapy
- Thermal laser photocoagulation
- Anti-VEGF therapy (Sigler, Randolph, Calzada, Wilson, & Haik, 2014).

1.5 Machine Learning (ML)

Machine learning (ML) is a discipline derived from artificial intelligence as machine learning algorithms allows the machine to achieve human like intellect (Das, Dey, Pal, & Roy, 2015). Machine learning procedures make predictions using exampled/ trained data which is fed into the ML algorithms. These algorithms not only learn the pattern or store and retrieve data but also perform generalization.

Data is trained using input features, if generalization is not achieved accurately the input features are modified and fed data again go through training step. Most commonly used types of ML are: neural networks, supervised and unsupervised ML (Alpaydin, 2004; Muhammad & Yan, 2015).

1.5.1 Unsupervised Machine Learning

Unsupervised machine learning is an optimization technique that self organizes itself based on the previously learned data. Architecture of unsupervised ML algorithm is portrayed in Figure 5.

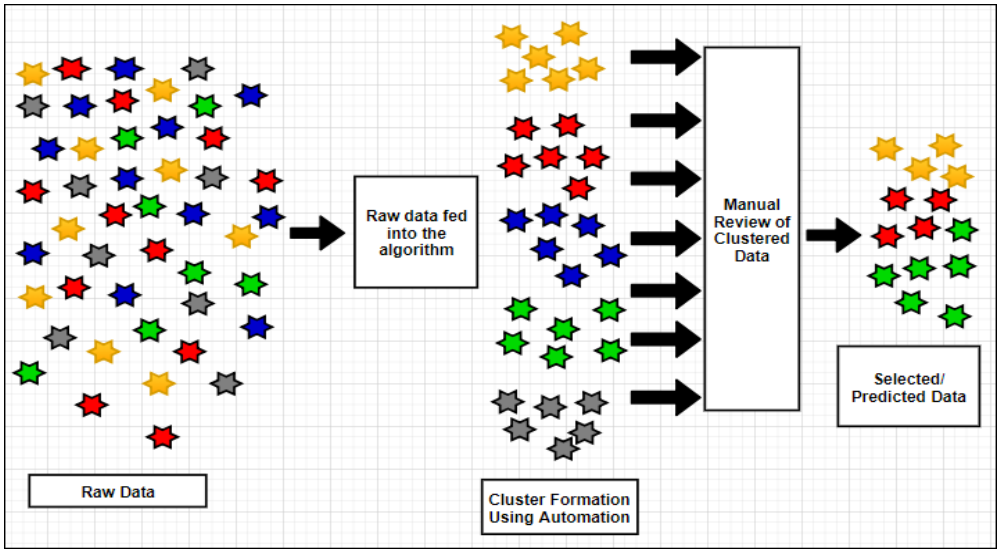

Figure 5 – A simple structure of unsupervised machine learning algorithm.

This type of learning is used for clustering problems of unlabelled, unclassified data. Interpretations are made based on raw data from which the unsupervised ML algorithm learns an input pattern (Das et al., 2015; Dey, 2016).

1.5.2 Supervised Machine Learning

In supervised machine learning, target labelled data is learned through a specific pattern to make predictions and classification of fed data is achieved. General steps of supervised ML described in Figure 6. Generally, data is separated into two sets, training and testing sets. Training data helps the algorithm find and learn patterns in the data and minimize the errors by computing and adjusting these errors. In training dataset, first step is to choose specific features with desired (expected) output values. These features can be binary, categorized or continuous (Kotsiantis, 2007). Training data also consists of noise or absent feature values and hence, next step is data pre-processing. When data is pre-processed, prediction accuracy measured by algorithm assessment step i.e. test set.

Machine learning algorithm learn the pattern from training set and utilize it on test set to classify and predict the computed data. This dataset is independent of trained data and is used to assess performance of model (Muhammad & Yan, 2015; Ripley, 1996).

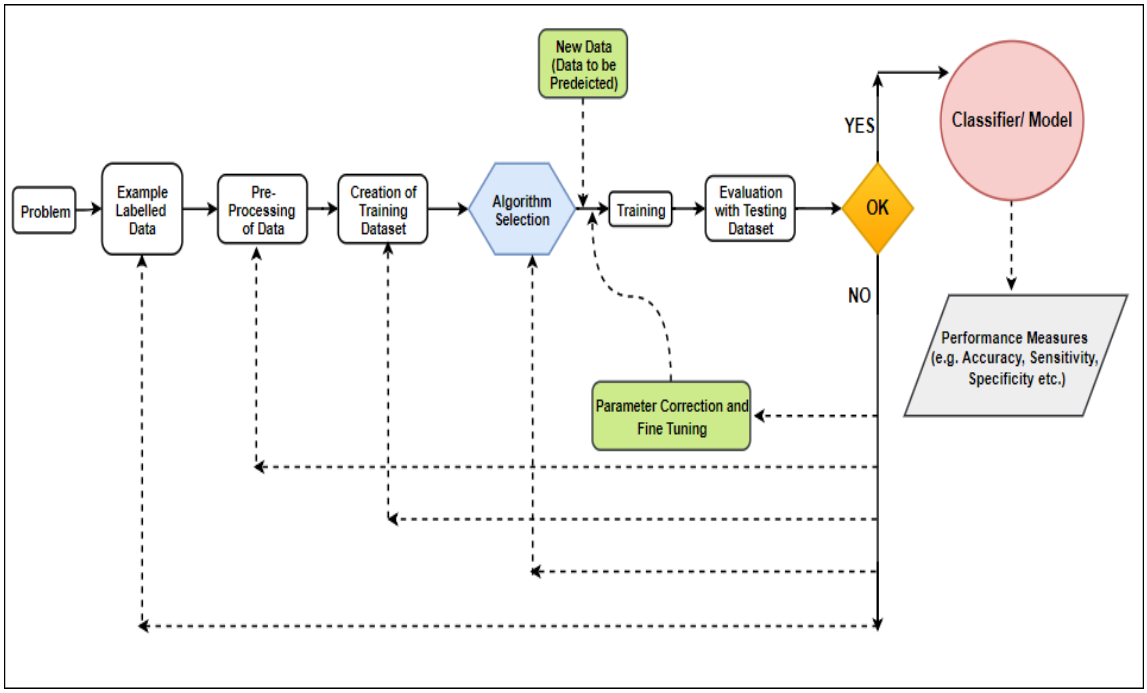

Figure 6 – Flow diagram explaining steps of supervised machine learning.

1.5.3 Neural Network

Neural networks or artificial neural networks (ANN) include interconnected simple processing units called artificial neurons. The neural network is wholly based on the idea of working of neurons as it converts inputs to outputs computationally. An illustration of a simple neuron structure is shown in Figure 7. Neuron is a functional component of nervous system. Human brain is made up of interlinked neuronal associations that receive and transmit information in the form of electrical stimuli.

A neuron is composed of axon, cell body, dendrites and axon terminals. A neuron makes connection to one or multiple neurons and transmit information through synapses. Neuronal signals control the activity of human brain using the transmitted information (Fasel, 2003).

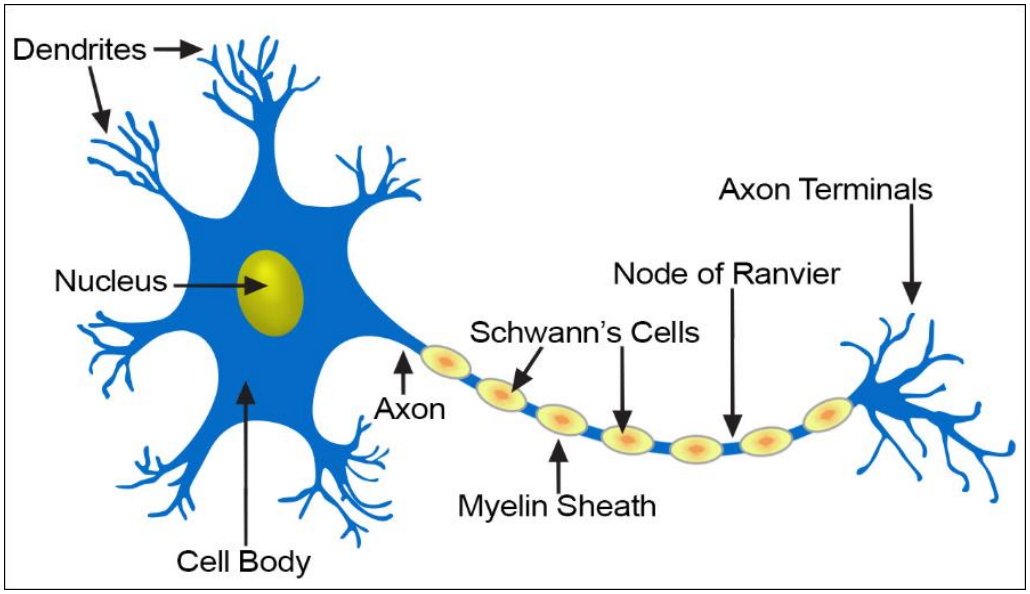

Figure 7 – A simple structure of a neuron cell. Main parts include axon, cell body, dendrites and axon terminals.

Neural network models are created on the basis of functionality of neurons in the Human brain. Neural networks are basically distributed into three main layers, input, hidden and output layer as depicted in Figure 8.

- *Input layer* gathers the numeric data and pass it for further computation into hidden layer.
- *Hidden layer* collects the data passed from input layer and further process it. Size and nature of the data determines the number of hidden layers in any neural network.
- Processed data is then fed to *Output layer* which provides the outcome of the problem (Dharwal & Kaur, 2016).

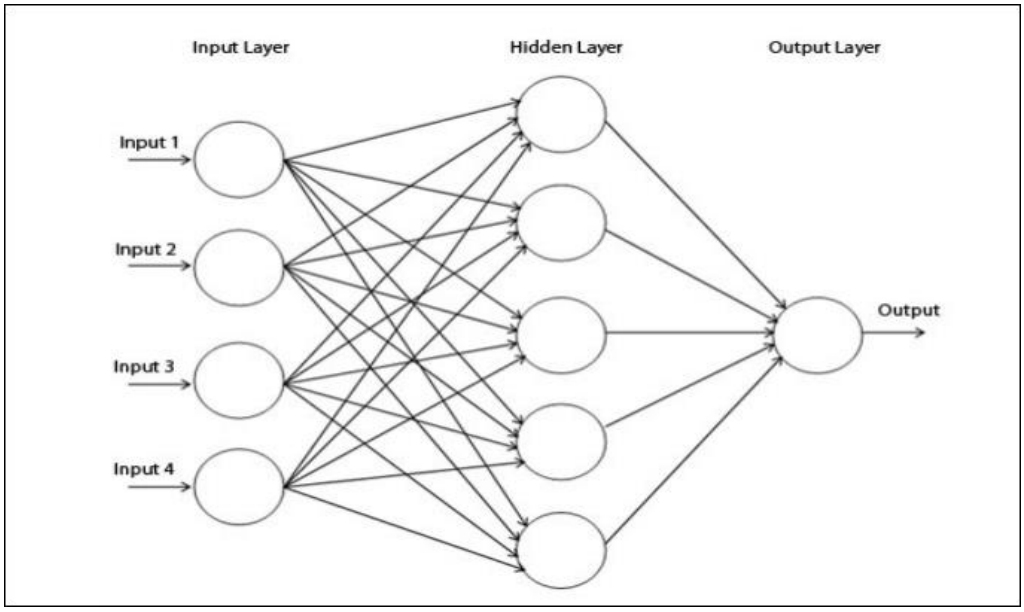

Figure 8 – Architecture of a simple neural network with input, hidden and output layers.

Several other components of neural networks include nodes, connectors, weights and activation function. Nodes of a neural network mimics the function of a biological neuron that transmit information through synapses to axons. Connectors of a NN acts as axons whereas weights represent the intensity of the input signal that are computed by mathematical functions referred to as activation function. Activation function of a neural network represents the activation rate of biological neuronal cells. An activation function in combination with sum of weighted inputs helps in determining the output (Dharwal & Kaur, 2016; Girish Jha, 2018; Kumar Jaiswal & Das, 2017).

1.6 Publicly Available Databases for Retinal Diseases

There are numerous publicly available retinal fundus image databases that have diverse features and purposes. In these databases, each retinal image has annotated data with ground truth (GT). Some of these public databases were investigated for this research that are listed below.

1.6.1 DIARETDB1- Standard Diabetic Retinopathy Database-Calibration Level 1

A widely accessible database for standardizing diabetic retinopathy diagnosis from digital retinal images. Database covers 89 annotated fundus images among which 5 pictures are normal and 84 consists of microaneurysms. 50◦ field-of-view digital fundus camera was used to take retinal images with a resolution of 1500×1152 pixels (T. Kauppi et al., 2007). Some of the pictures from this dataset are shown in figure 9.

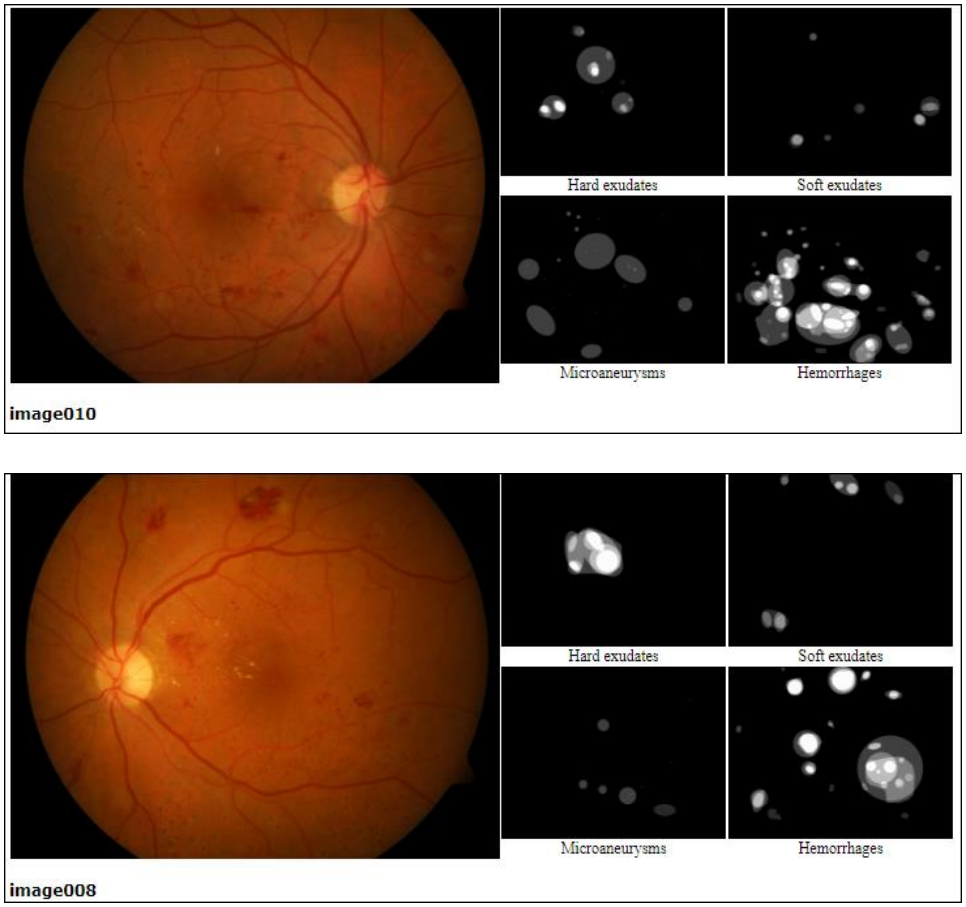

Figure 9 – (a) Image010 show signs of major retinal hemorrhage and microaneurysms. **(b)** Image008 has visible hemorrhages and hard exudates in DIARETDB1 Database.

1.6.2 DIARETDB0- Standard Diabetic Retinopathy Database-Calibration Level 0

The main goal of the database is to design a testing protocol which can be used as a paradigm for automated diabetic retinopathy detection systems. DIARETDB0 contain a sum of 130 colored fundus retinal images captured by 50◦ field-of-view digital fundus camera, some of images are illustrated in Figure 10. Dataset includes 20 normal images, 110 images have hard and soft exudates, microaneurysms, neovascularization and hemorrhages (Tomi Kauppi et al., 2006).

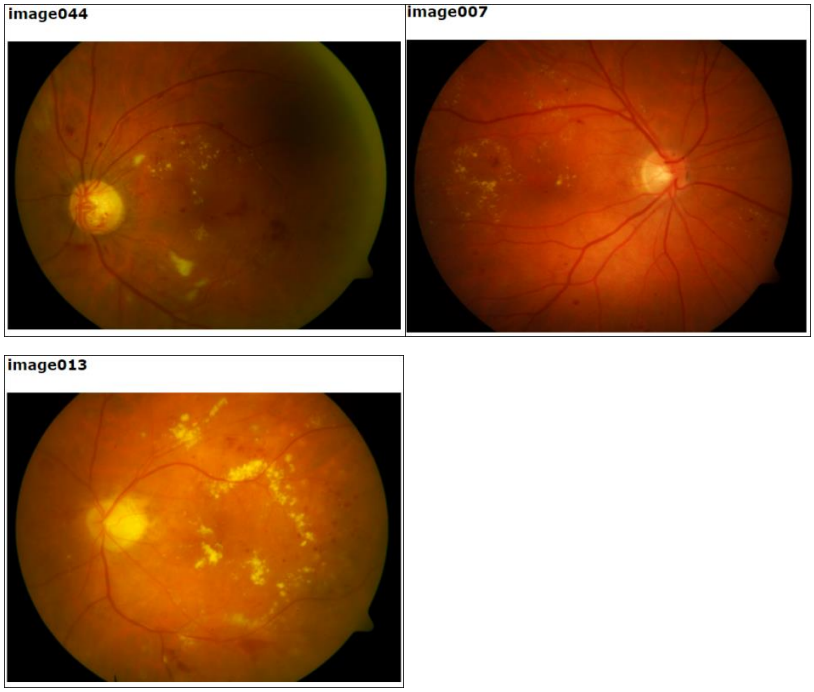

Figure 10 – DIARETDB0 images with ground truths. **(Image044) –** include red small dots, hemorrhages hard and soft exudates, neovascularisation. **(Image007) –** contains red small dots, hemorrhages and hard exudates. **(Image013) –** consist of red small dots, hemorrhages and hard exudates.

1.6.3 DRIVE Database

DRIVE stands for Digital Retinal Images for Vessel Extraction. This record is used to carry out comparative research centered on integration of retinal blood vessels. The pictures were attained from a diabetic retinopathy screening program in The Netherlands. 400 diabetic patients amongst 25-90 years of age took part in the diagnosis program (Staal, Abramoff, Niemeijer, Viergever, & van Ginneken, 2004). Database include a total of 40 images, 7 images have slight diabetic retinopathy signs, rest do not show any signs of DR. whole dataset is split into training and testing sets having 20 images each. All the images were taken using a Canon CR5 non-mydriatic 3CCD camera with a 45-degree field-of-view having 768 by 584 pixels.

1.6.4 DRIONS-DB

Digital Retinal Images for Optic Nerve Segmentation Database (DRIONS-DB) is a dataset used for research related to optic nerve head segmentation from images of retina (Carmona, Rincón, García-Feijoó, & Martínez-de-la-Casa, 2008). 110 colored digital retinal images that were obtained using coloured analogical fundus camera. Retinal images were digitized by HP-PhotoSmart-S20 elevated-resolution scanner in RGB setup with a resolution 600x400 and 8 bits/pixel.

1.6.5 HRF Image Database

High resolution fundus (HRF) image record was founded to promote automated findings on fundus images of retina (Budai, Bock, Maier, Hornegger, & Michelson, 2013). Dataset includes 15 images of healthy persons, 15 images of glaucomatous patients and 15 images of patients of diabetic retinopathy, only some are shown in Figure 11. Gold standard binary segmentation data, and masks that determine FOV of retinal images are also included in this dataset.

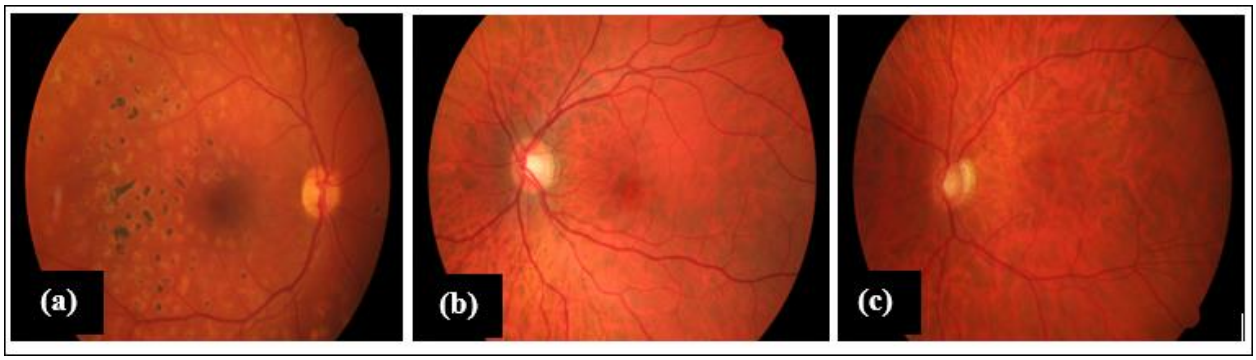

Figure 11 – HRF database images, **(a)** image showing signs of Diabetic Retinopathy, **(b)** image of a healthy retina and **(c)** image of Glaucoma patient.

1.6.6 STARE Database

Structured Analysis of the Retina (STARE) project was introduced in 1975 by Michael Goldbaum. Research related to this project, allows any system to spontaneously identify multiple sicknesses of the human retina using the digital fundus retinal images (A. D., V., & Goldbaum, 2000). Data in STARE database (depicted in Figure 12) includes:

- Using TRV-50 Fundus camera (Topcon Corp., Tokyo, Japan), ~400 colored retinal images were taken, at 35 degrees field with a resolution of 605x700 pixels.
- Provides information about clinically diagnosed diseases in each image
- All diseases have self-assigned codes
- Annotated 39 possible features/ symptoms information
- 40 labelled images of retinal blood vessels
- 10 labelled images of retinal artery and veins.
- 80 images including information about optic nerve detection with ground truth.

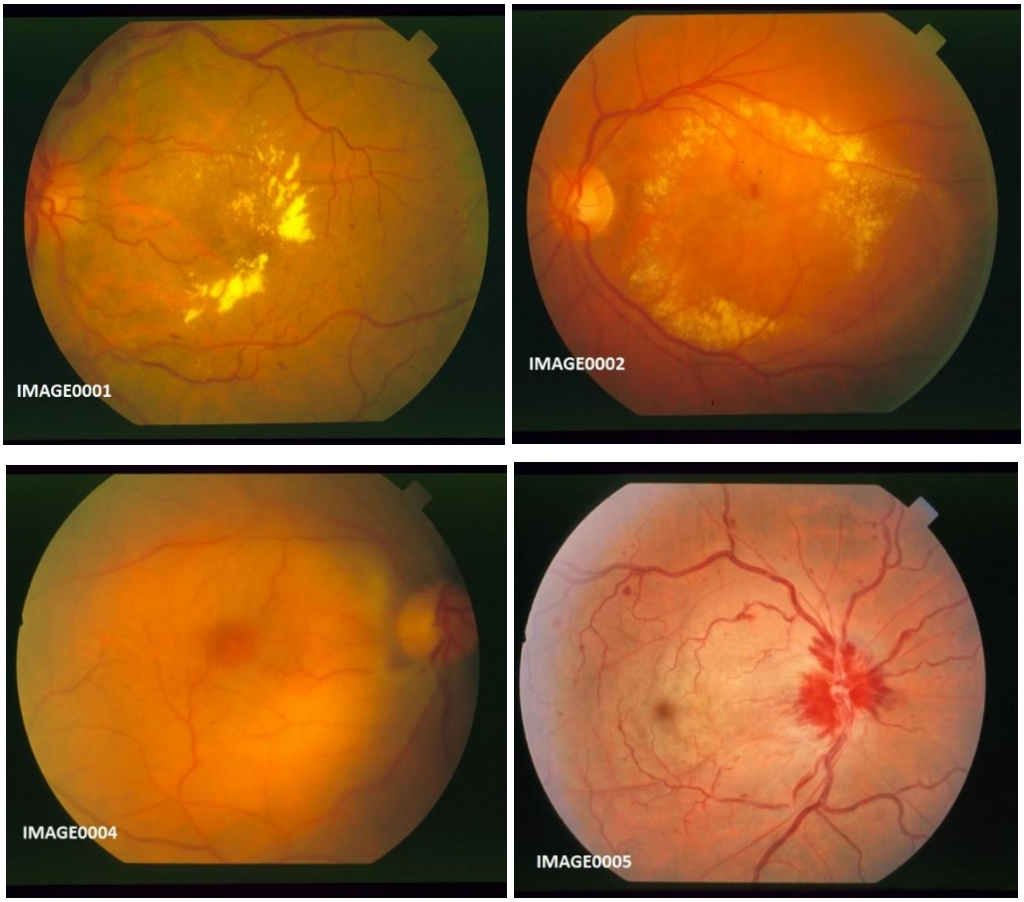

Figure 12 – STARE database images; (IMAGE0001) Background diabetic retinopathy, **(IMAGE0002)** Choroidal neovascularization and arteriosclerotic retinopathy, **(IMAGE0004)** Cilio-retinal artery occlusion or central retinal vein occlusion and **(IMAGE0005)** Central retinal artery and vein occlusion.

1.7 Machine Learning Based Classification

1.7.1 (1973)

Matsui et al. first published a technique to investigate the retinal images for blood vessel segmentation. Their methodology involved mathematical morphology digitization of fluorescein angiograms of the retina.

1.7.2 (1984)

Irregular structures of retina were first identified by Baudoin et al. in 1984 when they developed an image analysis approach to find microaneurysms using top-hat transform filter.

1.7.3 (1998)

In 1990s, striking change came forward by means of the advancement of digital retinal imaging and the development of filter-based image investigation procedures. In this research, the

algorithm was trained on 25 images set and tested on 160 images set to automatically diagnose retinal vascular diseases resulting from retinal hemorrhages. Neural network classification showed accuracy of 79% (Aleynikov & Micheli-Tzanakou, 1998).

1.7.4 (1999)

Sinthanayothin C *et.* al investigated the computer aided recognition of certain important landmarks (for instance optic disc (OD), retinal blood vessels and fovea) in 112 fundus photographs of the retina. Sinthanayothin C *et.* al used multilayer perceptron neural network for detection of blood vessels and fovea was identified by matching correlation in combination with general features of fovea. Area of higher intensity variation in neighbouring pixel values applied to identify the region of OD.

1.7.5 (2002)

In 2002 Alireza Osareh et. al investigated the automated classification and localisation of yellowish retinal exudates in Diabetic retinopathy using Fuzzy C-Means clustering approach for segmentation and classification of 60 colour retinal images attained from a non-mydriatic retinal camera. Optic disc (OD) was localised using template matching and least squares to better estimate OD boundaries. Obtained accuracies for exudate classification and OD localisation were 90.1 % and 90.7% respectively (Osareh, Mirmehdi, Thomas, & Markham, 2002).

Neural network (NN) and Support vector machine (SVM) classifiers were put into operation to investigate between the retinal exudate and non-retinal exudate classes. Results depicted that NN performed better than SVM but SVM provide a functional and more variable approach avoiding the problem of overfitting of data faced in NN approach (Osareh et al., 2002).

1.7.6 (2007)

Niemeijer M. et al. using computer aided system on 300 retinal fundus images, detected and differentiated cotton wool spots and exudates from drusen in diabetic patients. The method achieved 0.95 area under ROC curve, 0.95/0.88 sensitivity/specificity for bright lesions and for cotton wool spots, exudates and drusen 0.95/0.86, 0.70/0.93, and 0.77/0.88 sensitivity/specificity. Drawback of this study is limited quality of annotated images that affects optimal performance of the machine learning system.

1.7.7 (2008)

Chaum E et al. devised an automated novel content-based image retrieval method to diagnose retinal diseases that provided probabilistic predictions about the occurrence, severity, and

symptoms of retinal diseases from 395 retinal images. Achieved sensitivity for age related macular degeneration was between the range of 75% to 100%, for proliferative diabetic retinopathy extended from 75% to 91.7%, for non-proliferative diabetic retinopathy calculated accuracy was 75% to 94.7%. Overall specificity of the proposed method found to be 91.3%.

1.7.8 (2010)

Jaafar, H.F et al. depicted an computerized system for early diagnosis of hard and soft exudates that are among preliminary symptoms of diabetic retinopathy.

Coarse and fine segmentation techniques applied to retinal images taken from two publicly available retinal image databases i.e. *DIARETDB1, Drive* database and *Messidor* database, coarse segmentation outlined bright lesion boundaries using local variation operation while adaptive thresholding used for fine segmentation technique.

All bright lesions were segmented locally by split and merge method. Jaafar, H.F et al. calculated the exudate specificity at 99.3%, 99.4% accuracy and 89.7% sensitivity. The limiting factor for the proposed algorithm is that the system failed to differentiate between some non-exudate lesions and exudative lesions (Jaafar, Nandi, & Al-Nuaimy, 2010).

1.7.9 (2012)

In this study, investigation on diagnosis of diabetic retinopathy (DR) was made based on Probabilistic Neural network (PNN) and Support vector machine (SVM) with an accuracy of 89.60% and 97.608% respectively. SVM classified the proliferative and non-proliferative diabetic retinopathy better than PNN. This method diagnosed the DR at initial stages helping in early and efficient treatment (Priya & Aruna, 2012).

1.7.10 (2014)

This research presented SVM based classifier for optical coherence tomography (OCT) images of retinal diseases on a total of 45 subjects including three categories namely *(1)-normal, (2)-diabetic macular edema (DME)* and *(3)-age related macular degeneration in dry form (dry AMD).* Correctly identified cases for DME and dry AMD were 100% for both and 86.67% for normal category. Limitation of this study recognized to be that this algorithm is not intended for all types of manifestations of other retinal diseases (Srinivasan et al., 2014).

1.7.11 (2015)

In 2015, scientists explored three models of automated binary classification methods for diabetic retinopathy. Performance of Multilayer perceptron (MLP), Principal component

analysis (PCA) and Support vector machine (SVM) was compared resulting in 97% sensitivity, 95.7% correct classification cases of DR and 99% specificity. This study proposed that neural network SVM model represent better accuracy than simple NN model (Borkhade & Raut, 2015).

1.7.12 (2016)

In 2016 Gulshan V. et. al, studied the automated deep learning algorithm to diagnose diabetic macular edema and diabetic retinopathy using fundus retinal images. Deep convolutional NN was employed to a set of 128175 fundus images of the retina resulting in high sensitivity and specificity for referable diabetic retinopathy.

Limitation of this study was the grading criteria set by ophthalmologist graders and CNN was trained only for two disease categories missing certain other non-diabetic clinical landmarks (Gulshan et al., 2016).

1.7.13 (2017)

Choi JY et al. devised a deep learning convolutional neural network algorithm to automatically detect multiple retinal diseases using retinal images provided by STARE database. Dataset was divided into 10 disease categories; 1 normal and 9 disease categories.

Random forest transfer learning approach was applied constructed on VGG-19 architecture. 10 disease categories resulted in an accuracy of 30.5%, relative classifier information (RCI) of 0.052, and Cohen's kappa of 0.224. 3 disease categories revealed better performance with 0.283 RCI, 0.577 kappa and an accuracy of 72.8%.

Random forest transfer learning approach in combination with an ensemble classifier gave accuracy of 36.7%, 0.225 kappa and 0.053 RCI in the 10 retinal diseases. Limitation of this study included *(1)*- the poor performance of the automated system that was dependent on the amount of classes of diseases as the figure of classes increased, implementation of the system lowered, *(2)*- less number of retinal fundus images was not sufficient to be applied clinically.

1.8 Motivation for Current Study

Research has already been carried out on retinal diseases like recognition of arteries, veins, arterio-venous crossings, feature detection of blood vessel using optical and spatial properties of blood vessels, computer aided recognition and mapping of Drusen in Retinal Fundus images, automatic detection of micro aneurysms and its clinical evaluation, recognition of optic disc (OD), macula and age-related macular degeneration, using a computer based automatic method.

- *There is a constant need for the development of new automated methods to achieve better computer-based detection of multiple retinal diseases.*
- *Automated detection and vasculature analysis can help in implementing the screening programs for different retinal diseases like, diabetic retinopathy, micro-aneurysms.*
- *Machine learning can be furthered by supplementary training data sets, it may be valuable for detecting clinically important bright lesions, enhancing early diagnosis, and decreasing visual loss in patients with retinal diseases.*
- *This study can benefit the clinicians and researchers working in the field of imaging and ophthalmology for better automated diagnosis of such diseases.*

1.9 Objectives of Current Study

- Development of an automated diagnostic tool for identification of different retinal diseases using a single algorithm.
- Timely detection of diseases by image analysis.
- Comparing the efficiency of traditional machine learning algorithms with deep learning algorithms.

2 Methodology

This chapter details the procedure used to perform the NN based classification of diseases. The overall experimentation protocol is highlighted, and the various steps of the entire process are discussed briefly in the following sections.

2.1 Data Acquisition

Data was attained from STARE database in the form of colored retinal fundus images. ~400 raw images of human retina were captured using TRV-50 Fundus camera (Topcon Corp., Tokyo, Japan) at 35 degrees field with a resolution of 605x700 pixels.

2.1.1 Image Diagnosis

All images in the database have separate diagnosis and diagnosis codes assigned with the help of ophthalmologic experts as illustrated in Figure 13 and 14. Some images have one disease diagnosed by experts while some have two or more diagnosed diseases. Diagnosis codes were assigned to thirteen disease categories 14^{th} category included all other diseases with less number of images.

2.1.2 Feature Information

A total of ~400 text files corresponding to ~400 images in the dataset are present. In each file there are 44 numbers. These numbers signify features/manifestations found in each image. If a feature is present (it is indicated by number 2 and above 2) or if absent (indicated by number 1) in the text files. Hence, all manifestations were converted to binary data in **MATLAB 2017a** i.e. '**0**' showing absence of a feature and '**1**' if a feature is present.

Therefore, a total of 44 probable appearances were challenged to the experts during data collection and then decreased to 39 quantities throughout encoding, for this purpose a mapping file for all manifestation is available in the dataset shown in Figure 15.

```
im0001  7              Background Diabetic Retinopathy
im0002  13 9           Choroidal Neovascularization AND Arteriosclerotic Retinopathy
im0003  14             Drusen, large AND Geographic Atrophy RPE"
im0004  14 3           Cilio-Retinal Artery Occlusion OR Central Retinal Artery Occlusion
im0005  3 5            Central Retinal Artery Occlusion AND Central Retinal Vein Occlusion
im0006  14             Drusen
im0007  13 14 9 10     Choroidal Neovascularization AND Age Related Macular Degeneration AND ASR &HTR
im0008  13 14 9        Choroidal Neovascularization AND Age Related Macular Degeneration AND ASR
im0009  7              Background Diabetic Retinopathy
im0010  14             Histoplasmosis
im0011  13 14          Choroidal Neovascularization AND Histoplasmosis
im0012  14             Drusen
im0013  7              Background Diabetic Retinopathy
im0014  14             Nevus
im0015  14             Drusen
im0016  7              Background Diabetic Retinopathy
im0017  13             Choroidal Neovascularization
im0018  5              Central Retinal Vein Occlusion, compensated
im0019  5              Central Retinal Vein Occlusion
im0020  3 5            Central Retinal Artery Occlusion AND Central Retinal Vein Occlusion
im0021  8              Central Retinal Vein Occlusion
im0022  9              Arteriosclerotic Retinopathy
im0023  14             ????
im0024  14             Epiretinal Membrane??
im0025  5 9            Central Retinal Vein Occlusion AND Arteriosclerotic Retinopathy
im0026  5              Central Retinal Vein Occlusion
im0027  5              Central Retinal Vein Occlusion
im0028  6 9            Hemi-Central Retinal Vein Occlusion AND Arteriosclerotic Retinopathy
im0029  14             Unknown Diagnosis
im0030  0              Normal?
im0031  7              Background Diabetic Retinopathy
im0032  0              Normal
im0033  5              Central Retinal Vein Occlusion
im0034  13 14          Choroidal Neovascularization AND Age Related Macular Degeneration
im0035  14             Normal
```

Figure 13 – Diagnosis for each image present in STARE database.

Thirteen Diagnoses Considered

Diagnosis Number	Diagnosis	Abbreviation used
1	Hollenhorst Emboli	Emboli
2	Branch Retinal Artery Occlusion	BRAO
3	Cilio-Retinal Artery Occlusion	CRAO
4	Branch Retinal Vein Occlusion	BRVO
5	Central Retinal Vein Occlusion	CRVO
6	Hemi-Central Retinal Vein Occlusion	Hemi-CRVO
7	Background Diabetic Retinopathy	BDR/NPDR
8	Proliferative Diabetic Retinopathy	PDR
9	Arteriosclerotic Retinopathy	ASR
10	Hypertensive Retinopathy	HTR
11	Coat's	None
12	Macroaneurism	None
13	Choroidal Neovascularization	CNV

Figure 14 – Thirteen diagnosis codes assigned to diseases by STARE database.

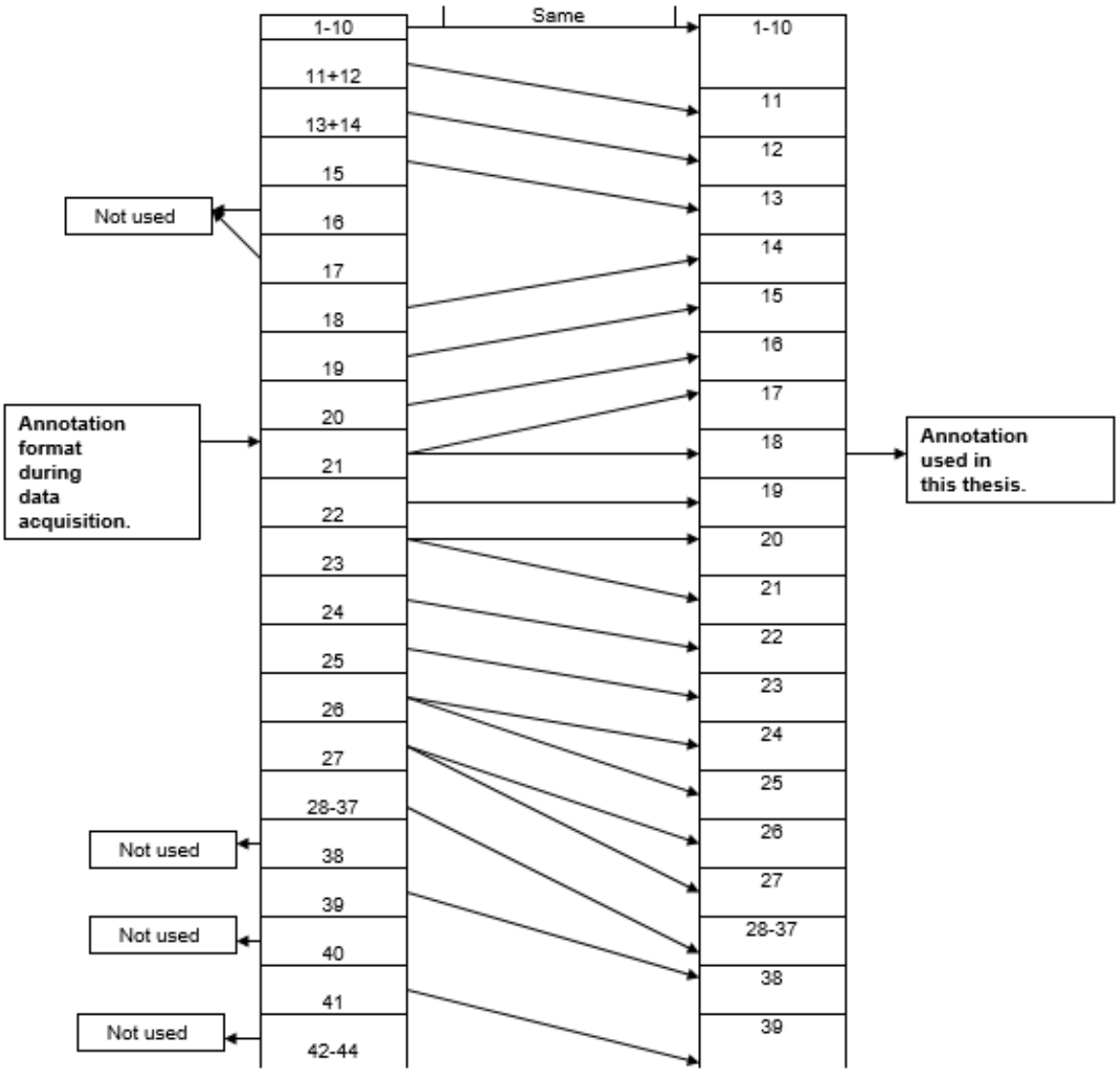

Figure 15 – Mapping of 44 manifestation into 39 manifestations.

2.1.3 Disease Information

On exploring the STARE database, a total of 41 disease categories were found while one category included images of normal retina.

Table 2 - STARE database contain a total of 41 diseases, this table provides information of diseases present.

Sr. No	Diseases	Sr. No	Diseases
1	Background Diabetic retinopathy	22	Myelinated nerve fibers
2	Choroidal Neovascularization	23	Asteroid hyalosis
3	CRAO	24	Epiretinal membrane
4	CRVO	25	Retinitis pigmentosa
5	Age related macular degeneration	26	Emboli, Non-hollenhorst
6	Retinitis	27	Frosted branch vascuopathy
7	Hypertensive retinopathy	28	Chorioretinal scar
8	Histoplasmosis	29	Choroidal hemangioma
9	Arteriosclerotic retinopathy	30	Tumor unknown
10	Macroaneurism	31	Optic nerve atrophy
11	Coat's disease, not isolated telangiectasia	32	Toxoplasmosis
12	HemiCRVO	33	Unknown diagnosis
13	BRVO	34	Myopia
14	Proliferative diabetic retinopathy	35	Choroidal melanoma
15	BRAO	36	Stellate maculopathy
16	Hollenhorst plaque	37	Vasculitis
17	Drusen	38	Optic atrophy
18	Emboli	39	Asteroud hyalosis
19	Nevus	40	Geographic Atrophy RPE
20	Patterned RPEopathy	41	HIV
21	RD (retinal detachment)		

2.2 Data Pre-processing

Collected data was preprocessed by applying two main steps.

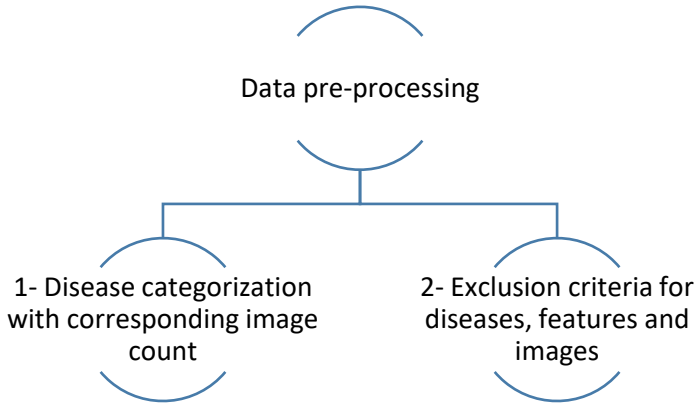

2.2.1 Disease Categorization with Corresponding Image Count

In reference to the clinical diagnosis provided in STARE database, uncategorized diseases were assigned separate numbers resulting in 41 diseases instead of 14. Images were counted for every disease in MATLAB, this led to the formation of exclusion criteria for diseases, features and images. All diseases were illustrated in Figure 16.

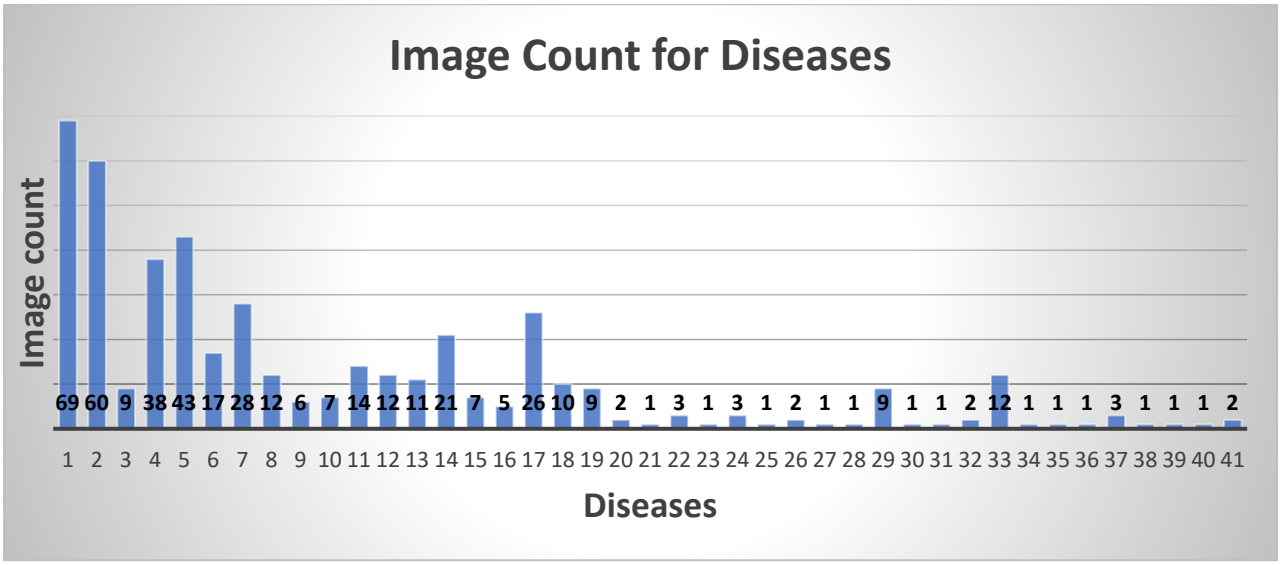

Figure 16 – Diseases represented on x-axis and image count for respective diseases is represented on y-axis.

2.2.2 Exclusion Criteria for Diseases, Images & Features

Two reduction criteria were set for all collected data. First, <5 image criterion was applied to the data. Secondly, < 50 % criterion was applied leading to exclusion of diseases, images and features as demonstrated in Figure 17 and 18.

2.2.2.1 <5 Images

Database contains 402 images, 41 diseases and 37 features, among 402 images only 311 images have valid information about features and diseases. 91 images were neglected due to improper diagnosis.

Due to exclusion of these inappropriate and not recommended diseases (according to database) 21 diseases were left. Out of the remaining 21 diseases, 2 categories (unknown diagnosis and choroidal hemangioma) were not used as recommended by the STARE project, leaving only 19 diseases, 37 features and 301 images.

2.2.2.2 < 50 % Occurrence of Feature Vs Disease

< 50% criteria when applied to 19 diseases, 15 features and 112 images were eliminated as a result we get 189 valid images for 22 features and 19 diseases. This criterion applied to 19 diseases.

WHY?

- To choose those discriminative features that are specific for a particular disease.
- Threshold value set to 9
- The features with > 9 occurrence in diseases were eliminated, resulting in 22 features. The features that were removed are feature number 6, 9, 11, 12, 13, 14, 17, 18, 21, 23, 24, 26, 27, 29, 31. For this purpose feature suppression mask was applied in MATLAB 2017a, as eliminated features equals to 0.
- There were some images in database that had only those features which were eliminated, hence those images were also removed.
- Due to the removal of these images, some diseases did not meet the < 5 Image criteria, in turn also eliminated leaving only 16 diseases, hence leaving valid 186 images and 16 diseases.

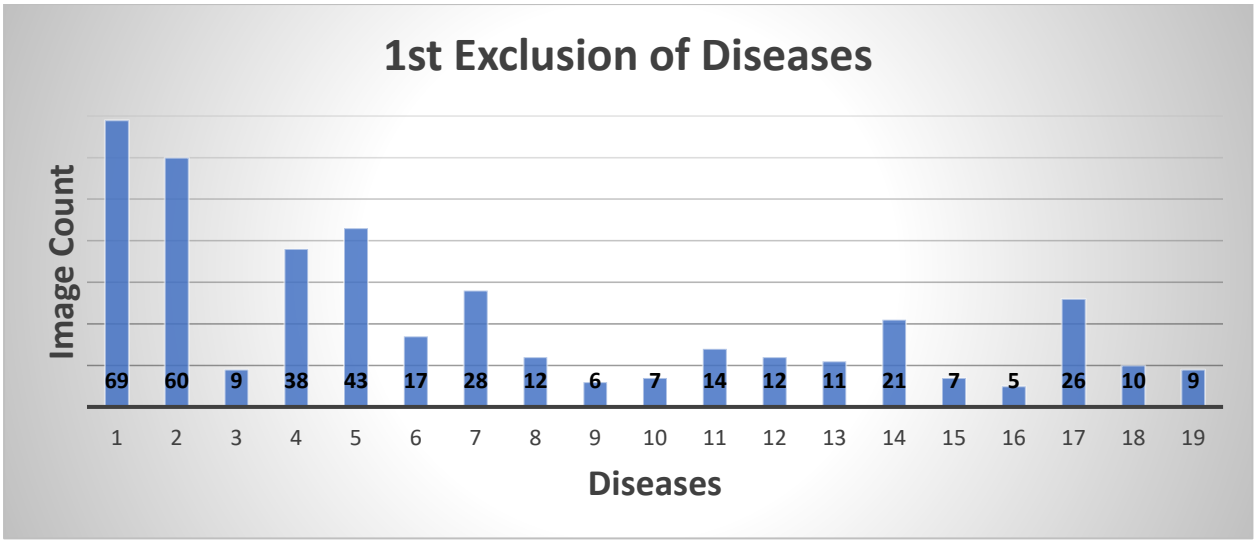

Figure 17 – First exclusion of diseases after two criteria were used.

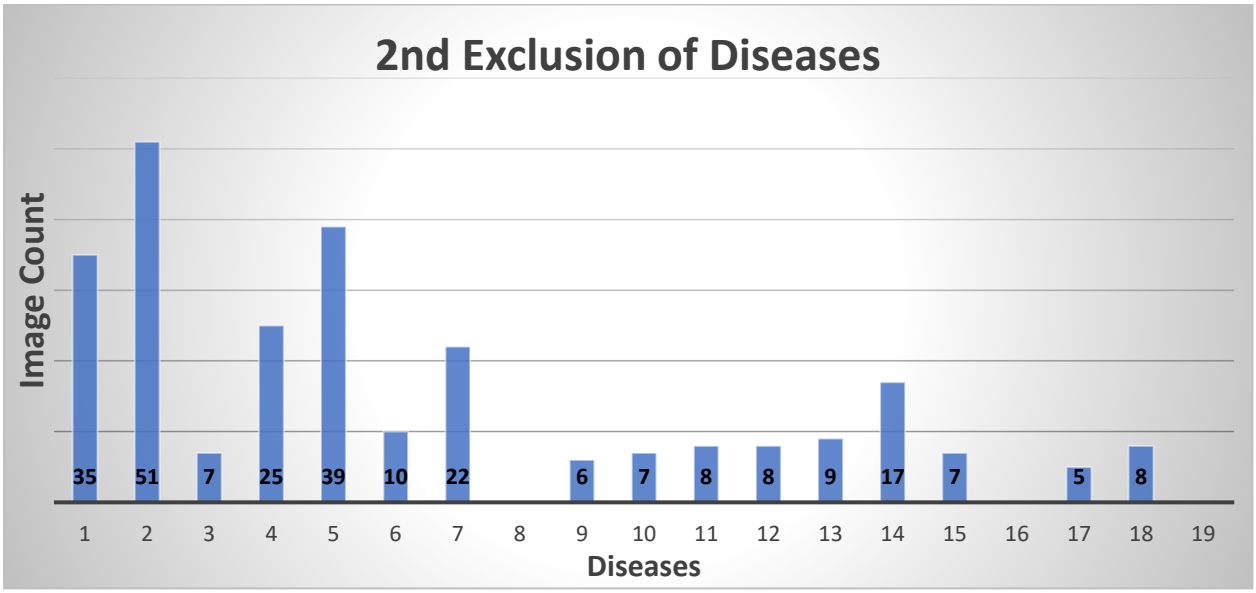

Figure 18 – Second reduction of diseases when both exclusion criteria were applied. Disease 8, 16 and 19 were removed using MATLAB 2017a.

Sixteen diseases and 186 images were finally selected to be further processed shown in Figure 19 and Table 3. Acquired data was then separated into training and testing samples using biased random sampling.

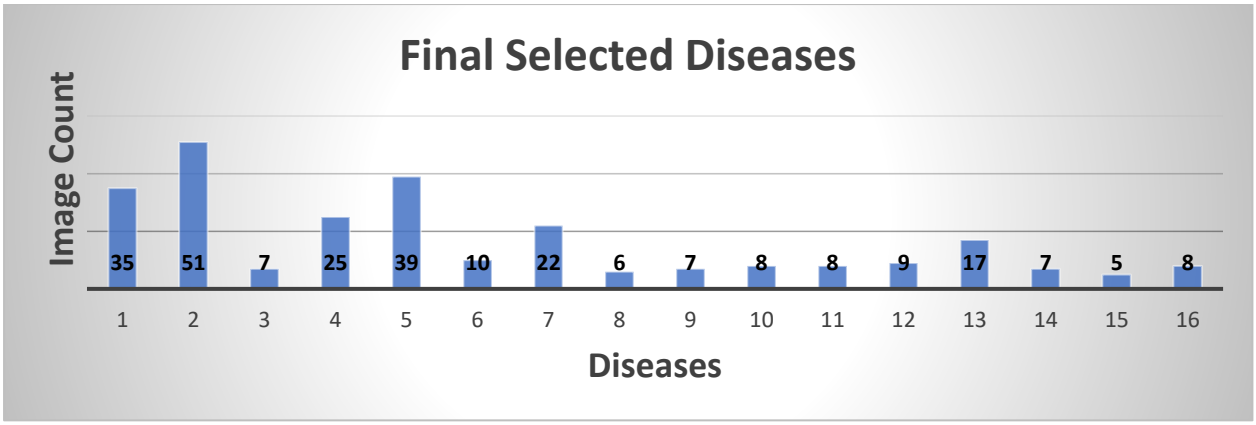

Figure 19 – 16 diseases with respective image count.

Table 3 – This table gives description of final selected 16 diseases.

Sr. No.	Disease Name	Sr. No.	Disease Name
1	Background diabetic retinopathy	**9**	Macroaneurism
2	Choroidal neovascularization	**10**	Coats' Disease
3	Central retinal artery occlusion	**11**	Hemi-central retinal vein occlusion
4	Central retinal vein occlusion	**12**	Branch retinal vein occlusion
5	Age related macular degeneration	**13**	Proliferative diabetic retinopathy
6	Retinitis	**14**	Branch retinal artery occlusion
7	Hypertensive retinopathy	**15**	Drusen
8	Arteriosclerosis retinopathy	**16**	Choroidal nevus

2.3 **Biased Random Sampling**

Biased random sampling is performed on the selected data and all data is separated into training and testing sets by 70 %, 30 % split.

- 70 % images are partitioned for training in ascending order of disease occurrences.
- Min number of occurrences are for disease no. 15 (i.e. 5 positive samples, 181 negative samples).
- total 130 images are separated for training (i.e. 70 % of total no. of images available).
- Remaining 56 images are separated for testing.

2.4 **Neural Network Design**

Current study involves a neural network comprising of following components:

- Total amount of features used as input - **22**
- Total amount of neurons in output layer - **16**
- No of hidden layers - **1**
- No of neurons in hidden layer - **20**
- Squishification functions used:
    - Sigmoid,
    - Arctan and
    - Gaussian

2.5 **Architecture of Neural Network**

Neural network design was based on 22 features, 16 disease categories and 186 images respectively. Architecture of NN is depicted in Figure 20.

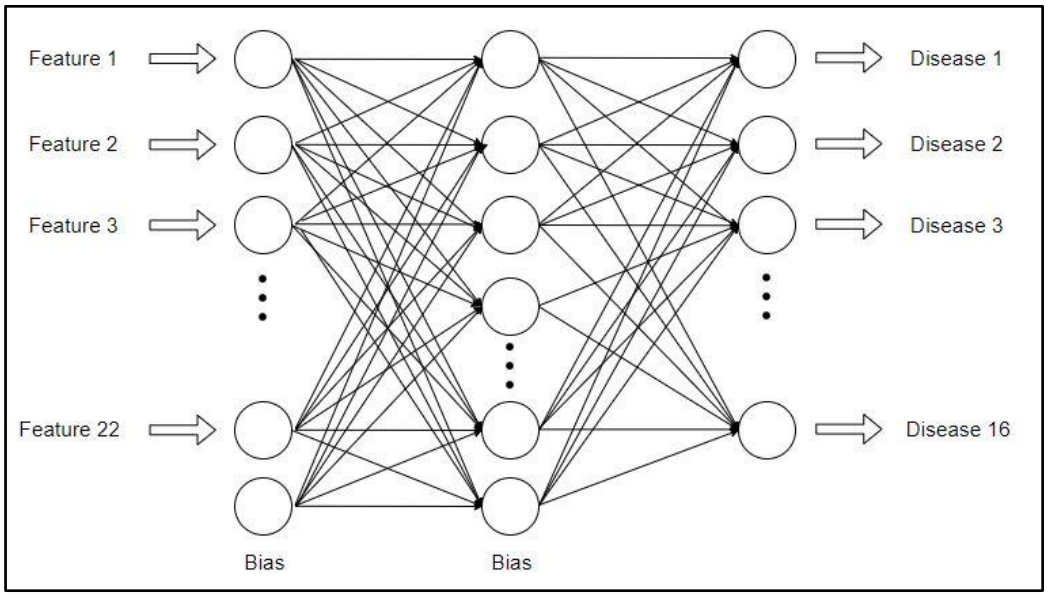

Figure 20 – Architecture of a neural network for retinal disease classification.

2.5.1 **Description of Synapses**

Synapses and weights of the neural network designed for this study were arranged and adjusted in the following order:

- 22 neurons in the first layer + 1 bias connected to 20 hidden layer neurons

- **Syn0 - (22+1) x 20 weights**

- 20 neurons in the hidden layer + 1 bias connected to 16 output layer neurons
  - **Syn1 - (20+1) x 16 weights**

2.6 Convergence

2.6.1 Forward Propagation of Neural network

In such neural networks, each layer provides input to the subsequent layer by activation of neurons/nodes. Firstly, input layer is activated, sums of the inputs are given to neurons of 1st layer of the NN followed by the activation of 1st layer. Next sums of input data are then provided to the 2nd layer followed by the activation of 2nd layer. By using the following formulas described process is performed:

L0(:, i) = X _ train (i,:)';	*% Activations of the input layer*
*Z1(:,i) = (horzcat(L0(:,i)',ones()) * Syn0)';*	% Sums to be given as input to neurons of first layer
L1(:,i) = neuron(Z1(:,i),0);	% Activations of the first layer
*Z2(:,i) = (horzcat(L1(:,i)',ones()) * Syn1)';*	% Sums to be given as input to neurons of second layer
L2(:,i) = neuron(Z2(:,i),0);	% Activations of the output layer

2.6.2 Cost Function and Back Propagation of Neural Network

Back propagation of a neural network for training its algorithm is performed by calculating the cost function of the entire network. Cost function means to find the squared error function for whole NN, then by estimating the error for all outputs and hidden layer neurons by using the outputs of last layer. Adjustment of weights is done based on the evaluated cost function and the learning rate.

- Cost function formula

$$C = \sum (L2 - y)^2$$

- Back propagation formulae

$$\frac{\partial C}{\partial w_{syn}} = \frac{\partial C}{\partial L2} \times \frac{\partial L2}{\partial Z2} \times \frac{\partial Z2}{\partial L1} \times \frac{\partial L1}{\partial Z1} \times \frac{\partial Z1}{\partial w_{syn}}$$

$$\frac{\partial C}{\partial w_{syn}} = \frac{\partial C}{\partial L2} \times \frac{\partial L2}{\partial Z2} \times \frac{\partial Z2}{\partial w_{syn}}$$

2.6.3 Gradient Descent and Update

Gradient descent is basically an optimization of parameters of cost function and helps in the choice of better cost function with minimum error. Gradient descent calculates a local (or global) minimum by allocating initial values to the factors and then iteratively keeps altering the given values that are proportional to the negative of the gradient of the cost function.

Enhancing amount of iterations improves the performance of the neural network by fine tuning the synapses. Gradient is then subtracted from previous synapse values

$$w_{syn} \coloneqq w_{syn} - \frac{\partial C}{\partial w_{syn}}$$

2.6.4 Iterations

Iteration of a neural network is the number of datasets needed to complete one epoch. While one epoch means that when whole dataset undergoes a forward or back propagation one time in a neural network algorithm. A total of 1000 iterations were performed for this study, to better tune the designed neural network and to attain better results.

2.7 Training Set

Training set continue to train data in neural network until cost function reaches a particular minimum. Training set included 130 images out of 186 total images; partitioned by biased random sampling in 70 %, 30 % split of whole data into training and testing sets. A total of three activation functions applied to the neural network.

2.7.1 Activation Functions

The most imperative unit in neural network assembly is the activation function. the selection of the squishification functions has vital effect on the network functioning. For our work, three activation functions were used.

2.7.1.1 Sigmoid NN

A sigmoid function is a non-linear activation function and it ranges between (0 to 1). Hence, used for such systems where we must predict the probability as an output. It is defined as:

$$s(x) = sigmoid(x) = \frac{1}{(1 + e^{-x})}$$

Where, *x* is input, *e* is exponent. *S(x)* is a continuous and differentiable entity. The derivative of the sigmoid pertaining to input x, is effortlessly evaluated as described in equation below:

$$s'(x) = (\frac{1}{1+e^{-x}}) \times (1 - \frac{1}{1+e^{-x}})$$

Derivative of a sigmoid function is frequently used for computing the weight information in training the neural network model with gradient descent (Han & Moraga, 1995).

2.7.1.2 Arctan NN

The arctan function constricts the input in the range $-\boldsymbol{\pi}/\mathbf{2}$ to $\boldsymbol{\pi}/\mathbf{2}$. It can differentiate better between similar input values. It is the inverse of tangent function and represented by the formulae:

$$f(x) = tan^{-1}(x)$$

Derivative of Arctan function is as follows:

$$f'(x) = \frac{1}{1+x^2}$$

2.7.1.3 Gaussian NN

Logarithm of a gaussian function is represented by a continuous bell-shaped curve. Output of a system is inferred on the probability of **0** or **1** in terms of a classification problem depending on the closeness of net input value to a selected average value. Gaussian ($\sigma = 0.7; \mu = 0$) function is explained by the equation as:

$$f(x) = \frac{1}{\sqrt{2\pi}\sigma^2} \times \exp(\frac{x^2}{2\sigma^2})$$

Gaussian function derivative is represented by a formula given below:

$$f'x) = (-\frac{x}{\sigma^2} \times \frac{1}{\sqrt{2\pi}\sigma^2} \times \exp(\frac{x^2}{2\sigma^2})$$

2.8 Testing Set

Testing set is used to evaluate the neural network prototype in an unbiased manner. Testing of a NN model is performed when training of data is complete. Testing set for this study include 56 images out of 186 images.

2.9 Evaluation

Evaluation of neural network model is performed using testing set data. For evaluation of the designated model, certain performance measures were completed on three activation function that provide quantitative information about the implementation of the proposed algorithm. These performance measures included accuracy, precision, recall, specificity and F1 score.

2.9.1 Accuracy

Accuracy of any system is the proportion of true results obtained. True positive cases are those which are properly recognized as having disease/feature, false positive cases are those that are incorrectly recognized as having disease/feature. Formulae for accuracy is:

$$Accuracy = TP + TN \div TP + FN + FP + TN$$

2.9.2 Sensitivity

Sensitivity correspondingly described as recall, is a measure of true positive cases, it accurately categorizes the cases actually having that disease. Sensitivity can be evaluated as:

$$Recall = TP \div TP + FN$$

2.9.3 Specificity

Specificity measures true negative cases, disease is not present but counted as a positive case, it can be calculated by:

$$Specificity = TN \div TN + FP$$

2.9.4 Precision

Precision is referred to as positive predictive estimate of samples. Precision also give information about true positive cases and calculated as:

$$Precision = TP \div TP + FP$$

2.9.5 F1 Score

F1 score is a measure of harmonic mean of precision and recall and it is computed as:

$$F1\ Score = 2.\ Precision.Recall \div precision + recall$$

2.10 **MATLAB Source Code**

The MATLAB Code used at the various stages of the complete protocol can be divided into major chunks. The code snippets are for sampling, neuron, NN design and training and testing.

The listing 1 below shows the code for generation of the datasets for training and testing. The original data is distributed through biased random sampling into 70% for training and 30% for testing.

The listing 2 shows the code snipped used to generate a single neuron in the neural network. Multiple types of neurons, with different activation functions (as discussed in the previous subsections) are used to create neural networks.

The third listing 3 shows the code snipped which uses the training data to train the neural networks with changing amount of features and then test the trained neural networks using the 30% testing data. Listing 3 also uses the testing data results to check for the various performance heuristics. The performance measures (as discussed in the previous subsections) are recorded and reported in the listing 3. This is used for further comparison between all different types of feature sets (reduced training sets through Principle Component Analysis) and the various activation functions of the neurons.

The Neural Network design is chosen to have 1 hidden layer based on prior knowledge and literature reviews. However a future study can vary the Neural Network architecture to observe the variation in the overall performance of the classifier.

```
% IMAGE VS FEATURE ANALYSIS FOR EACH DISEASE
testFeat = 26;
testDis = 7;
testChar = 'D';


finalFea = xlsread('finalFea.xls');
finalDis = xlsread('finalDis.xls');

% Diseases are remapped as following
% Old Disease Number        -       New Disease Number
%   1-17                    -           1-17
%   18                      -       Insufficient Cases
%   19,20                   -           18,19
%   21-clc
%   23                      -       Insufficient Cases
```

Listing 2.1 MATLAB Code Snippet for Biased Random Sampling

```
Features are mapped as following
% Old Feature Number        -       New Feature Number
%   1-37                    -           1-37
%   38-44    `              -           Not Used

redDis = zeros([402 19], 'logical');
redDis(:,1:17) = finalDis(:,1:17);
redDis(:,18:19) = finalDis(:,19:20);

redFea = zeros([402 37], 'logical');
redFea = finalFea(:,1:37);

[nImg, nFeat] = size(finalFea);
[nImg, nDis] = size(finalDis);

nIperD = sum(finalDis);
nIperF = sum(finalFea);


DFchart = zeros([length(finalDis) nFeat nDis], 'logical');

for k = 1:1:nDis
    for m = 1:1:length(finalDis)
        if(finalDis(m,k))
            DFchart(m,:,k) = finalFea(m,:);
        end
    end

end

scd = sum(sum(DFchart(:,:,testDis)));

dScat = zeros([2 scd]);

[rd, cd] = size(DFchart(:,:,testDis));

counter = 1;
for m = 1:1:rd
    for n = 1:1:cd
        if(DFchart(m,n,testDis))
            dScat(:,counter) = [m n]';
            counter = counter + 1;
        end
    end
end


% IMAGE VS DISEASE ANALYSIS FOR EACH FEATURE

nIperF = sum(finalFea);

FDchart = zeros([length(finalFea) nDis nFeat], 'logical');
```

```
for k = 1:1:nFeat
    for m = 1:1:length(finalFea)
        if(finalFea(m,k))
            FDchart(m,:,k) = finalDis(m,:);
        end
    end

end


scf = sum(sum(FDchart(:,:,testFeat)));

fScat = zeros([2 scf]);

[rf, cf] = size(FDchart(:,:,testFeat));

counter = 1;
for m = 1:1:rf
    for n = 1:1:cf
        if(FDchart(m,n,testFeat))
            fScat(:,counter) = [m n]';
            counter = counter + 1;
        end
    end
end

% Data Scatter Plots

% if(testChar == 'D' || testChar == 'd')
%     scatter(dScat(1,:),dScat(2,:),150,'x','red');
% end
%
% if(testChar == 'F' || testChar == 'f')
%     scatter(fScat(1,:),fScat(2,:),150,'x','blue');
% end

% DISEASE VERSUS FEATURE TABLE FOR REDUCED COUNTS
% FvD - Features / Diseases Table

FvD = zeros([37 19]);

for i = 1:1:402
    for j = 1:1:37
        if(redFea(i,j))
            FvD(j,:) = FvD(j,:) + redDis(i,:);
        end
    end
end

FvDcheck = zeros([37 19], 'logical');

for i = 1:1:37
    for j = 1:1:19
        if(FvD(i,j) > 0)
            FvDcheck(i,j) = 1;
        end
    end
end
```

```
FvDcheck shows if a feature and disease are present together
% Less than 50% check for reduction of features

redFea2 = zeros([402 22], 'logical');

% Features Mapping Sequence
% Old Features      -       New Features
% 1-5               -       1-5
% 7,8               -       6,7
% 10                -       8
% 15,16             -       9,10
% 19,20             -       11,12
% 22                -       13
% 25                -       14
% 28                -       15
% 30                -       16
% 32-37             -       17-22

% Features removed by 50% disease occurance check are;
% 6, 9, 11, 12, 13, 14, 17, 18, 21, 23, 24, 26, 27, 29, 31

redFea2(:,1:5)      = redFea(:,1:5);
redFea2(:,6:7)      = redFea(:,7:8);
redFea2(:,8)        = redFea(:,10);
redFea2(:,9:10)     = redFea(:,15:16);
redFea2(:,11:12)    = redFea(:,19:20);
redFea2(:,13)       = redFea(:,22);
redFea2(:,14)       = redFea(:,25);
redFea2(:,15)       = redFea(:,28);
redFea2(:,16)       = redFea(:,30);
redFea2(:,17:22)    = redFea(:,32:37);

% Feature Suppression mask
fsm = ones([1 37] , 'logical');
fsm(6) = 0;
fsm(9) = 0;
fsm(11:14) = 0;
fsm(17:18) = 0;
fsm(21) = 0;
fsm(23:24) = 0;
fsm(26:27) = 0;
fsm(29) = 0;

fsm(31) = 0;

frm = ~fsm;

for i = 1:1:402
    maskFea(i,:) = redFea(i,:).*fsm;
end

F = (sum(redFea'))';
M = (sum(maskFea'))';

redDis2 = redDis;
```

```
for i = 1:1:402
    if(M(i) == 0)
        redFea2(i,:) = zeros([1 22], 'logical');
        redDis2(i,:) = zeros([1 19], 'logical');
    end
end

% Removing diseases with less than 5 valid images
% These are Diseases 8, 16 and 19

redDis3 = zeros([402 16], 'logical');
redDis3(:,1:7)      = redDis2(:,1:7);
redDis3(:,8:14)     = redDis2(:,9:15);
redDis3(:,15:16)    = redDis2(:,17:18);

% Final Datasets

validImg = zeros([402 1],'logical');

temp = sum(redDis3');

for i=1:1:402
    if(temp(i) > 0)
        validImg(i) = true;
    end
end

nImg = sum(validImg);
IvF = zeros([nImg 22], 'logical');
IvD = zeros([nImg 16], 'logical');

sweep = 1;

for i = 1:1:402
    if(validImg(i))
        IvF(sweep,:) = redFea2(i,:);
        IvD(sweep,:) = redDis3(i,:);
        sweep = sweep + 1;
    end
end

% The Matrices IvF and IvD are the training / testing Matrices
% IvF -> Input Matrix for training / testing Features for Valid Images
% IvD -> Output Matrix for training  / testing Diseases for Valid Images

DiseaseCount = 16;

totalSamplesPerDisease = 186;

positiveSamplesPerDisease = sum(IvD);

pIndexPerDisease = zeros([max(positiveSamplesPerDisease) DiseaseCount]);
% A value of 0 in the pIndexPerDisease corresponds to no image

sweepCounter = ones([1 16]);
```

```
for i = 1:1:totalSamplesPerDisease
    for j = 1:1:DiseaseCount
        if(IvD(i,j))
            pIndexPerDisease(sweepCounter(j),j) = i;
            sweepCounter(j) = sweepCounter(j) + 1;
        end
    end
end

mxLine = positiveSamplesPerDisease;
mxRepVal = max(mxLine) + 1;
minIndex = 0;
minVal = 0;

totalTrainingSamples = floor(0.7*totalSamplesPerDisease);
totalTestingSamples = totalSamplesPerDisease - totalTrainingSamples;

trainingSamples = zeros([totalTrainingSamples 1]);
trainingIndex = 1;

testingSamples = zeros([totalTestingSamples 1]);
testingIndex = 1;

trainingPositiveSamplesCountPerDisease =
floor(0.7*positiveSamplesPerDisease);
testingPositiveSamplesCountPerDisease = positiveSamplesPerDisease -
trainingPositiveSamplesCountPerDisease;

for i = 1:1:DiseaseCount
    if(testingIndex > totalTestingSamples)
        break;
    end
    [minVal, minIndex] = min(mxLine);
    rTrainSample =
datasample(pIndexPerDisease(1:minVal,minIndex),trainingPositiveSamplesCo
untPerDisease(minIndex),'Replace',false);
    rTestSample =
setdiff(pIndexPerDisease(1:minVal,minIndex),rTrainSample);

    crossCheckTrain = ismember(rTrainSample, trainingSamples);
    crossCheckTest = ismember(rTrainSample, testingSamples);

    for j = 1:1:length(crossCheckTrain)
        if(~(crossCheckTrain(j)||crossCheckTest(j)))
            trainingSamples(trainingIndex) = rTrainSample(j);
            trainingIndex = trainingIndex + 1;
        end
    end

    crossCheckTrain = ismember(rTestSample, trainingSamples);
    crossCheckTest = ismember(rTestSample, testingSamples);
```

```
    for k = 1:1:length(crossCheckTest)
        if(~(crossCheckTrain(k)||crossCheckTest(k)))
            testingSamples(testingIndex) = rTestSample(k);
            testingIndex = testingIndex + 1;
        end
        if(testingIndex > totalTestingSamples)
            break;
        end
    end
    mxLine(minIndex) = mxRepVal;
end

allSamples = 1:1:totalSamplesPerDisease;
remainingSamples = setdiff(allSamples,trainingSamples);
remainingSamples = setdiff(remainingSamples,testingSamples);

trainingSamples(trainingIndex:end) = remainingSamples;

testingSamples = sort(testingSamples);
trainingSamples = sort(trainingSamples);

%clearvars -except IvF IvD trainingSamples testingSamples

% Partitioning Training and Testing Data

TrainingIvF = zeros([0 0],'logical');
TestingIvF = zeros([0 0],'logical');

TrainingIvD = zeros([0 0],'logical');
TestingIvD = zeros([0 0],'logical');

for i=1:1:186
    if(ismember(i,trainingSamples))
        TrainingIvF(end+1,:) = IvF(i,:);
        TrainingIvD(end+1,:) = IvD(i,:);
    else
        TestingIvF(end+1,:) = IvF(i,:);
        TestingIvD(end+1,:) = IvD(i,:);
    end
end

clearvars -except TestingIvD TestingIvF TrainingIvD TrainingIvF
```

```
% Sigmoid Function

% function Y = neuron(X,d)
%     if(d)
%         Y = 1./(1 + exp(-X)).*(1-1./(1 + exp(-X)));
%     else
%         Y = 1./(1 + exp(-X));
%     end
% end

% % ReLU Function
% function Y = neuron(X,d)
%     if(d)
%         Y = 1.*(X>0) + 0.*(X<0);
%     else
%         Y = X.*(X>0) + 0.*(X<0);
%     end
% end

% Arctan Function tanh
% function Y = neuron(X,d)
%     if(d)
%         Y = 1./(X.^2 + 1);
%     else
%         Y = atan(X);
%     end
% end

% Softplus function
% function Y = neuron(X,d)
%     if(d)
%         Y = 1 - tanh(X).^2;
%     else
%         Y = tanh(X);
%     end
% end

function Y = neuron(X,d)
    s = 0.7;
    if(d)
        Y = ( -X ./ (s^2) ) .* (1/sqrt(2*pi*s*s)) .* exp( - X.^2 /
(2*s^2) ) ;
    else
        Y = (1/sqrt(2*pi*s*s)) .* exp( - X.^2 / (2*s^2) ) ;
    end
end
```

Listing 2.2 MATLAB Code Snippet for a Neuron

```
% Neural Network Training Algorithm

% The Neural Network we will use for our case is defined in neuron
% and the input layer has 22 perceptrons for 22 features.


X_train = double(TrainingIvF);
Y_train = double(TrainingIvD);

X_test = double(TestingIvF);
Y_test = double(TestingIvD);

[nTr, nX] = size(X_train);  % Neurons in the input layer
[nTs, nY] = size(Y_test);   % Neurons in the output layer
nH = 20;                    % Neurons in the hidden layers
nRep = 1000;               % Number of training repititions

% Synapses Design
Syn0 = rand([nX+1 nH]);     % Input Layer + bias term
Syn1 = rand([nH+1 nY]);     % Output Layer + bias term

% Training Neural Network

nIteration = 1000;
dRecord = 10;
nRecord = nIteration/dRecord;

Syn0Stack = zeros([size(Syn0) nIteration/dRecord]);
Syn1Stack = zeros([size(Syn1) nIteration/dRecord]);

cross = 1;

for iteration = 1:1:nIteration

    % Forward Propagation
    for i = 1:1:nTr
        L0(:,i) = X_train(i,:)';                          % Activations of
the input layer
        Z1(:,i) = (horzcat(L0(:,i)',ones()) * Syn0)';      % Sums to be
given as input to neurons of first layer
        L1(:,i) = neuron(Z1(:,i),0);                    % Activations of
the first layer
        Z2(:,i) = (horzcat(L1(:,i)',ones()) * Syn1)';      % Sums to be
given as input to neurons of second layer
        L2(:,i) = neuron(Z2(:,i),0);
    end

    Cost = (L2 - Y_train').^2;
    CostAvg = mean(Cost')';
```

Listing 2.3 MATLAB Code Snippet for NN Design and Training/Testing

```
    if(mod(iteration,dRecord) == 0)
        disp(fprintf('Iteration No. %f Error is:
%d',iteration,sum(CostAvg)));
        Syn0Stack(:,:,cross) = Syn0;
        Syn1Stack(:,:,cross) = Syn1;
        cross = cross + 1;
    end
    % Calculating Deltas - Chain Rule form

    dCdSyn0 = zeros(size(Syn0));
    dCdSyn1 = zeros(size(Syn1));

    % First Layer Synapses
    for i = 1:1:nTr
        for j = 1:1:nX
            for k = 1:1:nH
                dCdSyn0(j,k) = dCdSyn0(j,k) + (1/nTr) * sum ( 2 *
(L2(:,i) - Y_train(i,:)') .* neuron(Z2(:,i),1) .* Syn1(k,:)' *
neuron(Z1(k,i),1) * L0(j,i));
            end
        end
    end

    for i = 1:1:nTr
            for k = 1:1:nH
                dCdSyn0(nX+1,k) = dCdSyn0(nX+1,k) + (1/nTr) * sum ( 2 *
(L2(:,i) - Y_train(i,:)') .* neuron(Z2(:,i),1) .* Syn1(k,:)' *
neuron(Z1(k,i),1) * 1);
            end
    end

    % Second Layer Synapses

    for i = 1:1:nTr
        for j = 1:1:nH
            for k = 1:1:nY
                dCdSyn1(j,k) = dCdSyn1(j,k) + (1/nTr) * sum ( 2 *
(L2(:,i) - Y_train(i,:)') .* neuron(Z2(:,i),1) .* L0(j,i));
            end
        end
    end

    for i = 1:1:nTr
            for k = 1:1:nY
                dCdSyn1(nH+1,k) = dCdSyn1(nH+1,k) + (1/nTr) * sum ( 2 *
(L2(:,i) - Y_train(i,:)') .* neuron(Z2(:,i),1) .* 1);
            end
    end

    Syn0 = Syn0 - dCdSyn0;
    Syn1 = Syn1 - dCdSyn1;
end
```

```
Layer1 = horzcat(X_test,ones([nTs 1]));
SumZ1 = zeros([nTs nH 100]);
Layer2 = zeros([nTs nH+1 100]);
SumZ2 = zeros([nTs nY 100]);
Layer3 = zeros([nTs nY 100]);

split = zeros([1 100]);

Y = zeros([nTs nY 100]);

for i = 1:1:100
    for j = 1:1:nTs
        SumZ1(:,:,i) = Layer1*Gaus_Syn0Stack(:,:,i);
        Layer2(:,:,i) = horzcat(neuron(SumZ1(:,:,i),0) , ones([nTs 1]));
        SumZ2(:,:,i) = Layer2(:,:,i)*Gaus_Syn1Stack(:,:,i);
        Layer3(:,:,i) = neuron(SumZ2(:,:,i),0);
    end
end

Y_pred = zeros([nTs nY 100]);
Y_split = zeros([1 100]);

for i = 1:1:100
    Y_split(1,i) = ( max(max(Layer3(:,:,i))) + min(min(Layer3(:,:,i))) )
/ 2;
end

for i = 1:1:100
    Y_pred(:,:,i) = 1.*(Layer3(:,:,i) >= Y_split(1,i)) +
0.*(Layer3(:,:,i) < Y_split(1,i));
end

Acc = zeros([16 100]);
Pre = zeros([16 100]);
Rec = zeros([16 100]);
Spe = zeros([16 100]);
F1 = zeros([16 100]);

Fp = zeros([16 100]);
Fn = zeros([16 100]);
Tp = zeros([16 100]);
Tn = zeros([16 100]);
```

```
for i = 1:1:nTs
    for j = 1:1:nY
        for k = 1:1:100
            if( Y_test(i,j) )
                if( Y_pred(i,j,k) )
                    Tp(j,k) = Tp(j,k) + 1;
                else
                    Fn(j,k) = Fn(j,k) + 1;
                end
            else
                if( Y_pred(i,j,k) )
                    Fp(j,k) = Fp(j,k) + 1;
                else
                    Tn(j,k) = Tn(j,k) + 1;
                end
            end
        end
    end
end

Acc = (Tp + Tn) ./ (Tp + Tn + Fp + Fn);
Pre = Tp ./ (Tp + Fp);
Rec = Tp ./ (Tp + Fn);
Spe = Tn ./ (Tn + Fp);

F1 = 2 * Pre .* Rec ./ (Pre + Rec);

for i = 1:1:16
    for j = 1:1:100
        if( (Acc(i,j) == inf) || isnan(Acc(i,j)) )
            Acc(i,j) = 0;
        end

        if( (Pre(i,j) == inf) || isnan(Pre(i,j)) )
            Pre(i,j) = 0;
        end

        if( (Rec(i,j) == inf) || isnan(Rec(i,j)) )
            Rec(i,j) = 0;
        end

        if( (Spe(i,j) == inf) || isnan(Spe(i,j)) )
            Spe(i,j) = 0;
        end

        if( (F1(i,j) == inf) || isnan(F1(i,j)) )
            F1(i,j) = 0;
        end

    end
end
```

3 Results

Results for the proposed neural network model for correct classification of retinal diseases evaluated based on number of iterations versus performance metrics of NN. Performance of three different activation functions were compared and the function providing best performance was chosen.

3.1 Data Visualization of Training and Testing Data

Firstly, training and testing sets were separated based on biased random sampling technique in MATLAB 2017a. Training and testing data was visualized as illustrated in Figure 21.

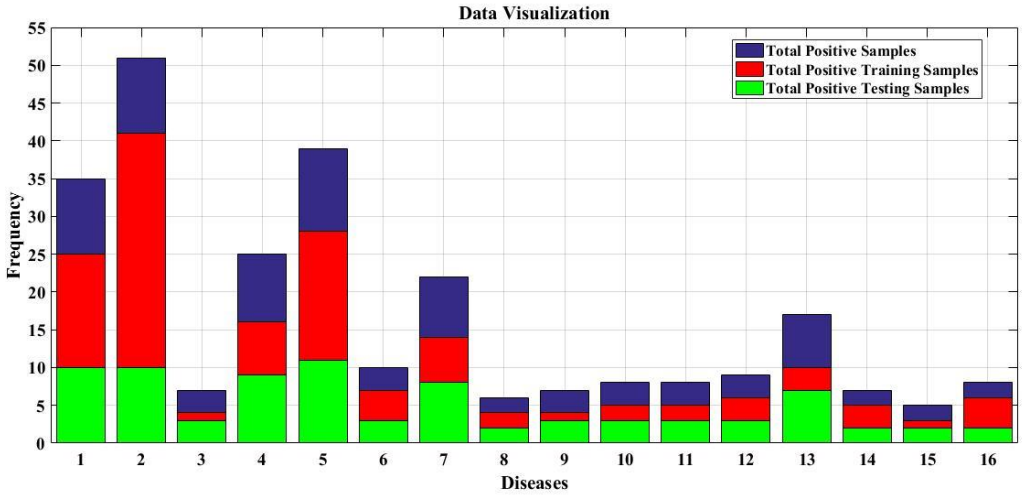

Figure 21 – This graph is plotted between disease samples and their respective frequency and shows the division of retinal images into training and testing sets, blue color represents total number of positive samples, red color shows all positive training samples while green color shows all positive samples for testing set.

3.1.1 Training Sample Percentages

Sampling technique for positive training samples of neural network model was observed by two different ways and the technique giving best trend was selected:

1. *Random sampling technique*
2. *Biased random sampling technique*

A graph displaying training sample percentages against respective diseases was plotted in MATLAB 2017a, is shown in Figure 22.

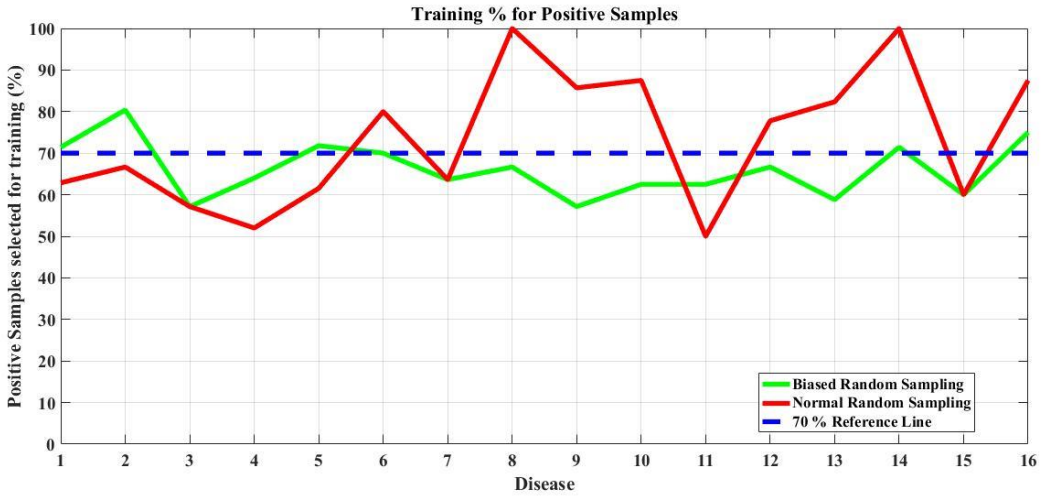

Figure 22 – This picture explains the trend observed for normal random sampling (red line) and biased random sampling (green random sampling) for positive samples selected for training of NN and respective diseases. Blue dotted line represents 70 % reference line that depicts 70 %, 30 % split into training and testing set.

3.2 Iteration Vs Performance of Activation Functions

Overall 1000 Iterations were performed for tuning Neural Networks based on all 3 activation functions (Sigmoid, Arctan, Gaussian). The Sigmoid (Logistic) Activation Function based NN did not go into overfitting and was only fine-tuned.

3.2.1 Sigmoid Neural Network

Accuracy for Sigmoid NN was estimated for 16 diseases (‘0’ if disease is absent and ‘1’ if disease is present), 22 features (‘0’ if feature is absent and ‘1’ if feature is present) and 186 images was 0.71 at 100 iterations, 0.82 at 200 iterations and 0.92 at 500 iterations with 0.95 specificity. Performance table for Sigmoid NN for all performance metrics is given below in Table 4.

Table 4 – This table describes accuracy, precision, specificity, recall and F1 score evaluated for several iterations.

Sr. No.	Iteration	Accuracy	Precision	Recall	Specificity	F1 Score
1.	10	0.12	0.10	0.2	0.14	0.2
2.	100	0.71	0.04	0.27	0.72	0.08
3.	200	0.82	0.06	0.28	0.88	0.08
4.	500	0.92	0.09	0.22	0.95	0.12

Diseases with more number of images revealed better performance. Different trends for five performance measures were observed for sigmoid activation function across 1000 iterations as illustrated in Figure 23.

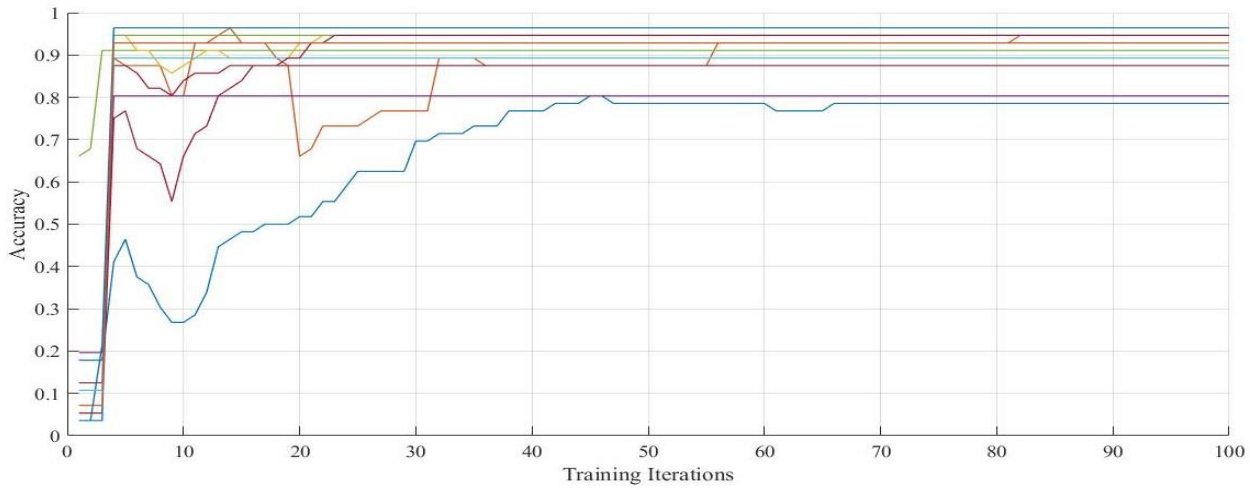

Figure 23 – Graph is plotted between accuracy on y-axis and 1000 iterations on x-axis (number 10 = 100, 20 = 200, 30 = 300…….100 = 1000 on x-axis). Different color of lines signifies 16 diseases respectively.

F1 score is used in binary classification problems. F1 score or F- measure is obtained by taking harmonic mean of precision and recall. F-score is used for testing the accuracy of a system as shown in Figure 24.

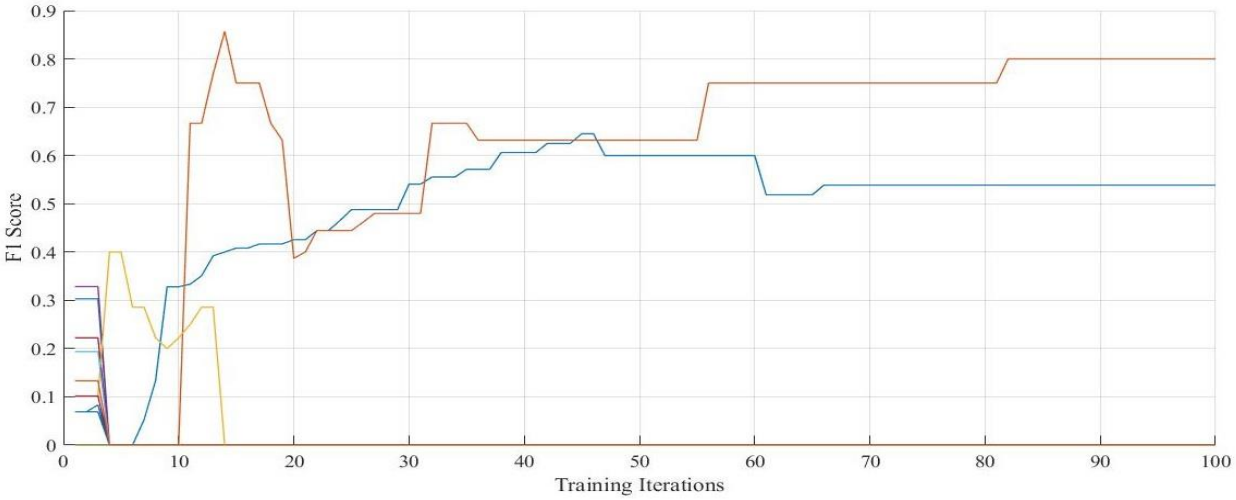

Figure 24 – F1 score for the designated NN model is plotted between F1 score and number of iterations, highest F1 score can be seen at 500 iterations (number 10 = 100, 20 = 200, 30 = 300…….100 = 1000 on x-axis).

Sigmoid based NN precision was evaluated for all 16 diseases. Precision is referred to as positive predictive values and shows the exactness and refinement while estimating model performance as depicted in Figure 25.

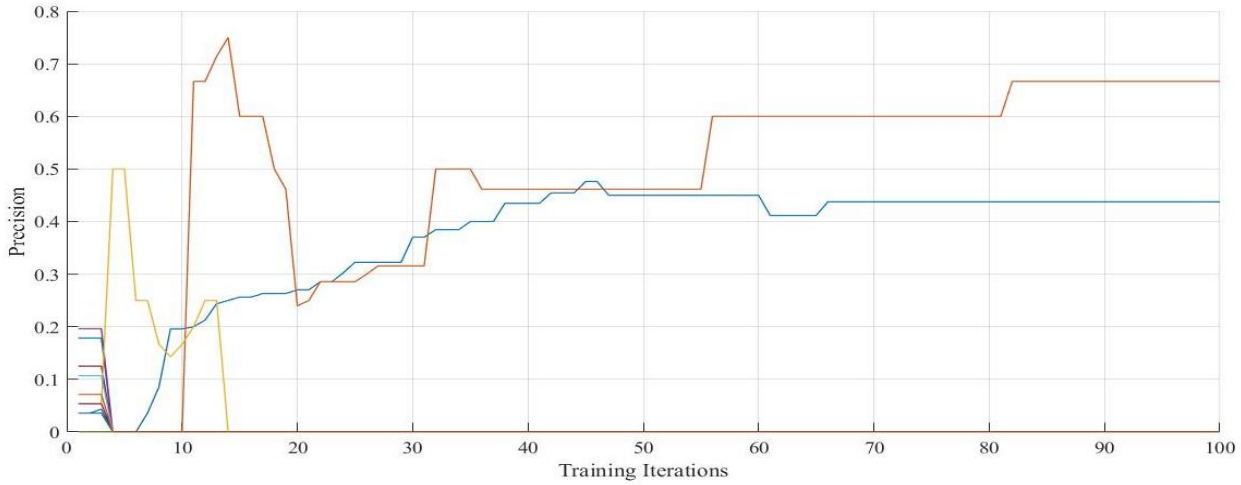

Figure 25 – This picture shows the precision trends of 16 diseases across 1000 iterations (number 10 = 100, 20 = 200, 30 = 300…….100 = 1000 on x-axis).

Precision and recall are applied in pattern recognition and classification problems. Recall is also defined as sensitivity of a system. Recall for sigmoid NN is shown in Figure 26.

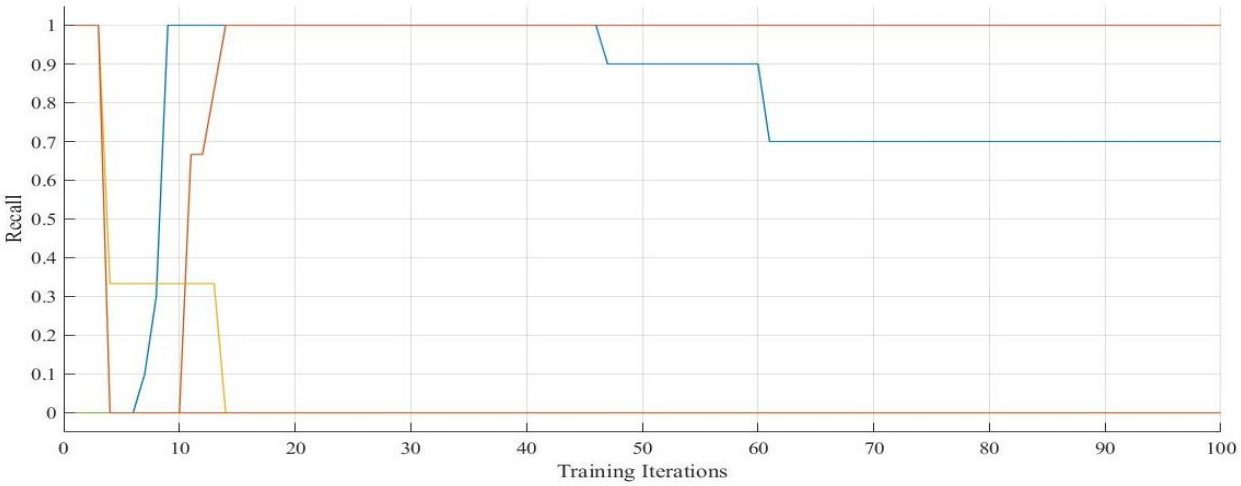

Figure 26 – Trends of all diseases for Recall of the system are shown across 1000 iterations (number 10 = 100, 20 = 200, 30 = 300…….100 = 1000 on x-axis).

Specificity is the calculated rate of true negative samples that are correctly recognized. For Sigmoid NN, specificity results of selected retinal diseases are shown in Figure 27.

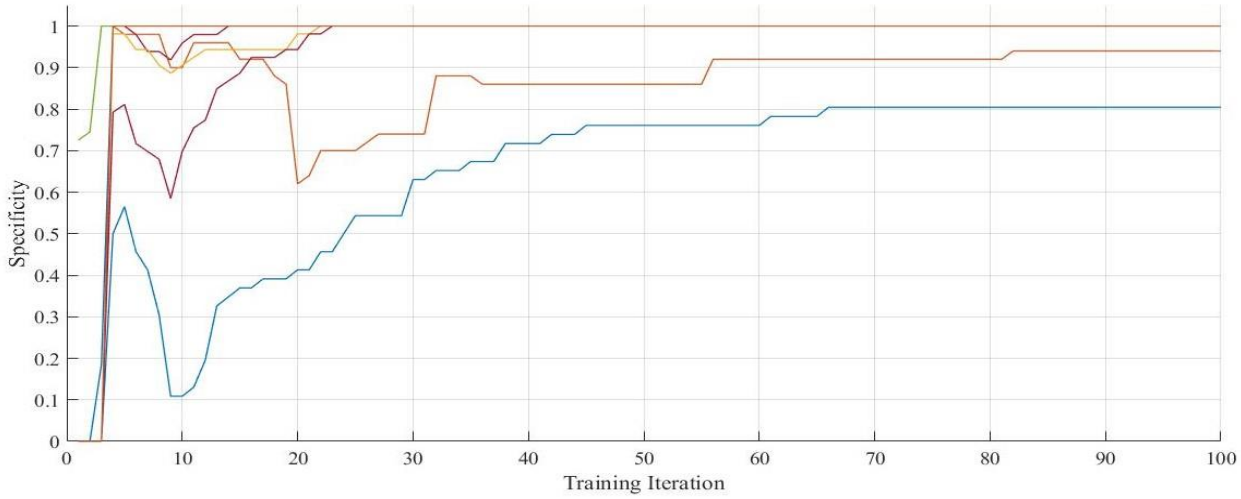

Figure 27 – Specificity was evaluated for 16 selected retinal diseases across 1000 iterations (number 10 = 100, 20 = 200, 30 = 300…….100 = 1000 on x-axis).

1.1.1 Arctan Neural Network

The Tan^{-1} Activation Function based NN was tuned within first 100 iterations and was over-fitting afterwards. Performance of Arctan based NN was poor in terms of all performance metrics i.e. accuracy, precision, F1 score, recall and specificity described in table 5.

Table 5 – Performance table for Arctan neural network.

Sr. No.	Iteration	Accuracy	Precision	Recall	Specificity	F1 Score
1.	10	0.50	0.08	0.67	0.53	0.2
2.	100	0.85	0.05	0.68	0.78	0.08
3.	200	0.66	0.92	0.36	0.58	0.19
4.	500	0.46	0.12	0.72	0.39	0.18

When Tan^{-1} activation function was applied in neural network, data for all diseases, features and images showed overfitting hence, mediocre performance was recorded for Arctan based neural network as shown in Figure 28.

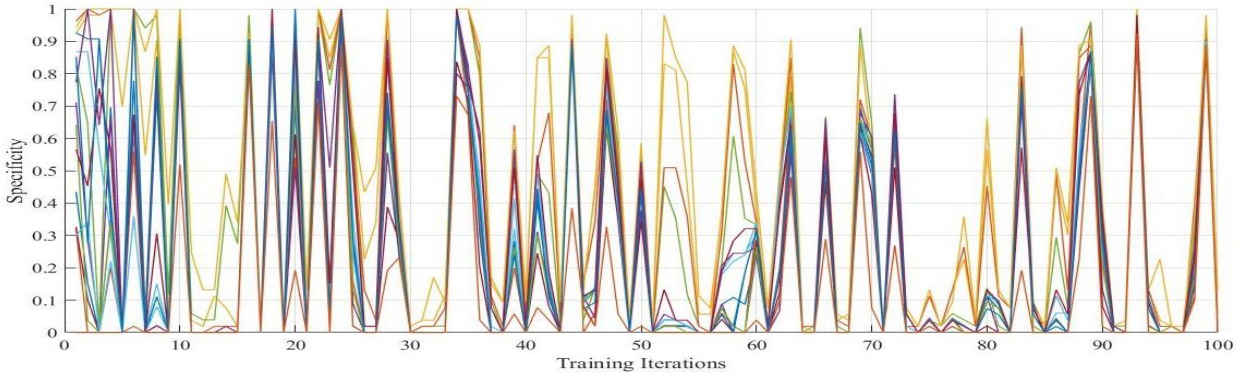

(a) Arctan Specificity

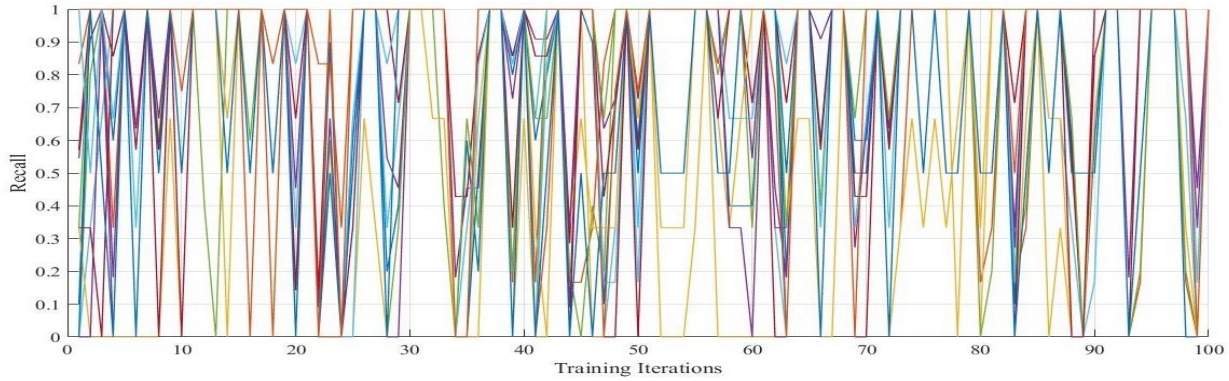

(b) Arctan Recall

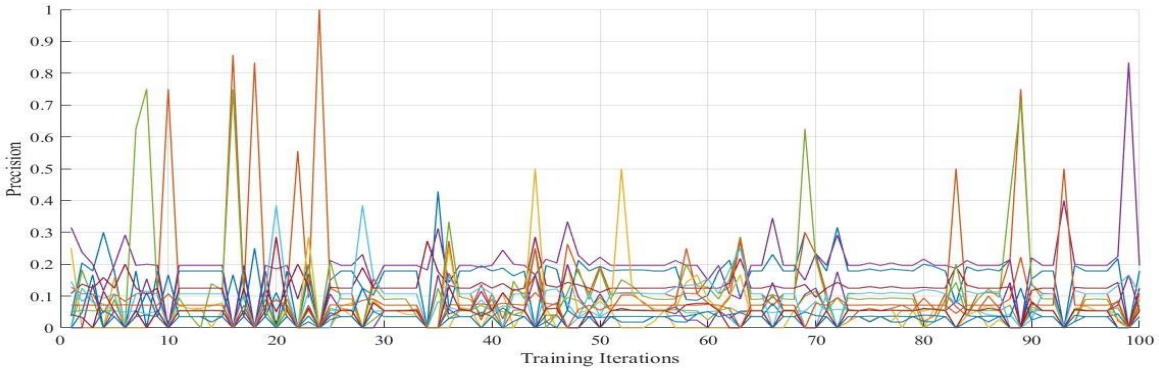

(c) Arctan Precision

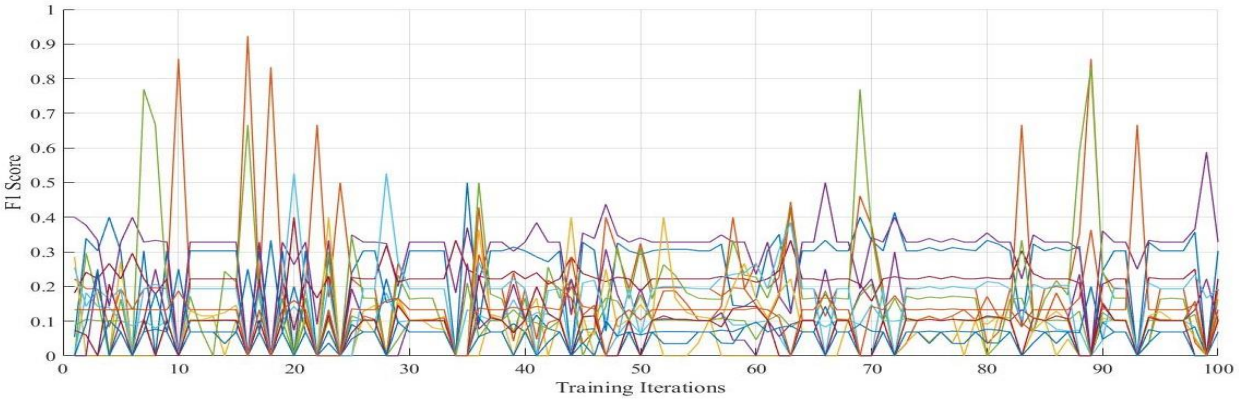

(d) Arctan F1 score

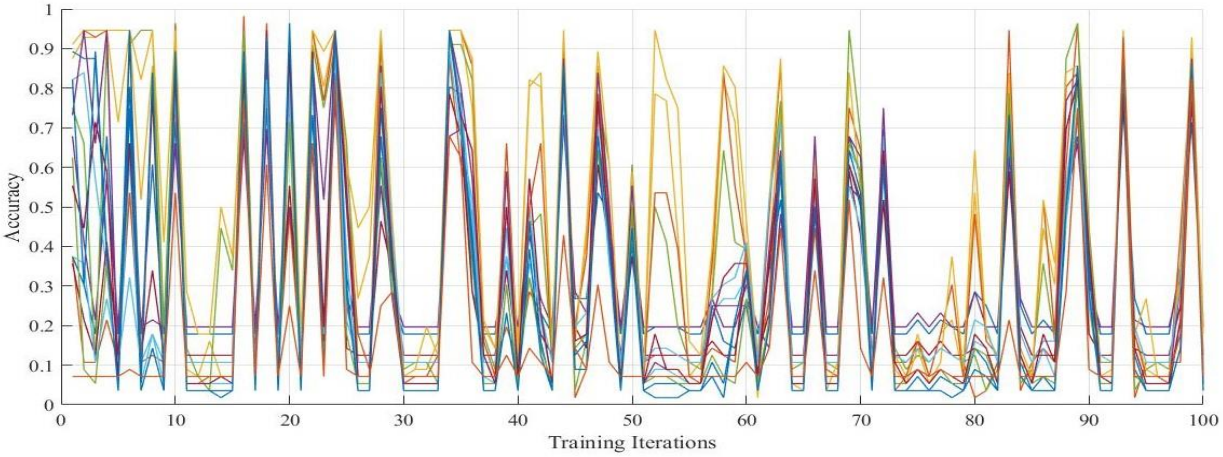

(e) Arctan Accuracy

Figure 28 – This figure illustrates accuracy, precision, specificity, recall and F1 score for Tan^{-1} based NN. All performance measures resulted in overfitting of the data across 1000 iterations (number 10 = 100, 20 = 200, 30 = 300…….100 = 1000 on x-axis).

1.1.2 Gaussian Neural Network

The Gaussian Activation Function based NN was tuned within **550** iterations and was over-fitting afterwards. Performance table for Gaussian based neural network is explained in table 6.

Table 6 – Performance table for Gaussian based NN.

Sr. No.	Iteration	Accuracy	Precision	Recall	Specificity	F1 Score
1.	10	0.86	0.09	0.02	0.95	0.03
2.	100	0.88	0.22	0.32	0.96	0.08
3.	200	0.92	0.30	0.48	0.96	0.13
4.	500	0.90	3.12	0.43	0.92	0.11

Gaussian based NN performed better than Arctan NN and in terms of precision Gaussian activation function performance was considered best among all three activation functions. Accuracy for Gaussian function was 0.90 at 500 iterations and 3.12 precision at 500 iterations. Performance trends presented in Figure 29 below.

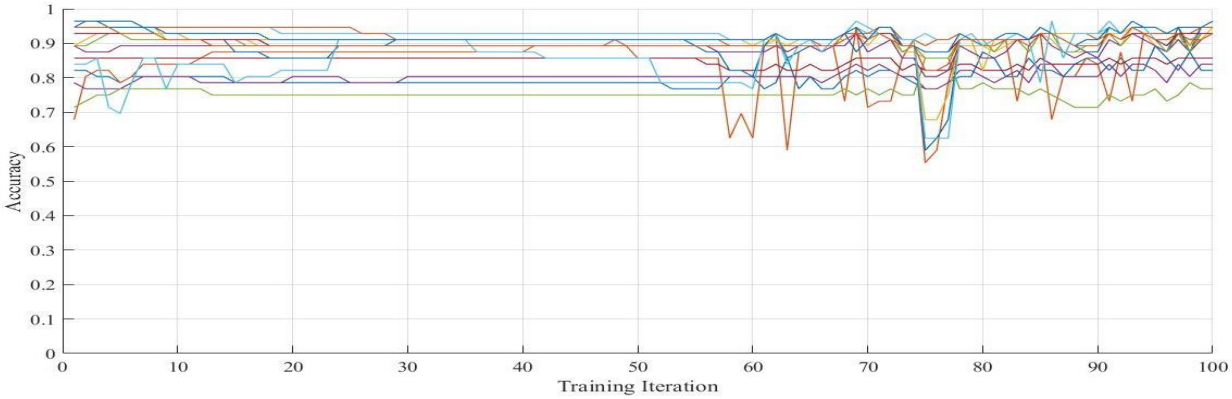

(a) Gaussian NN Accuracy

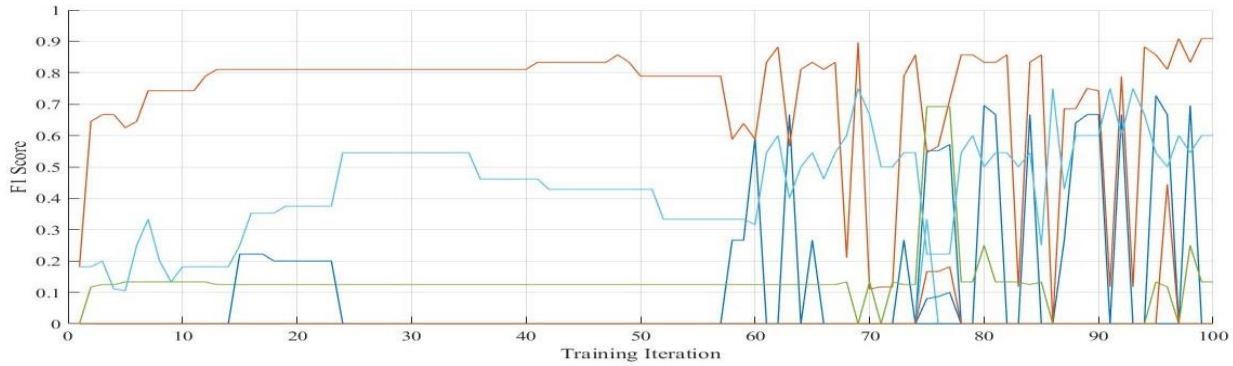

(b) Gaussian NN F1 score

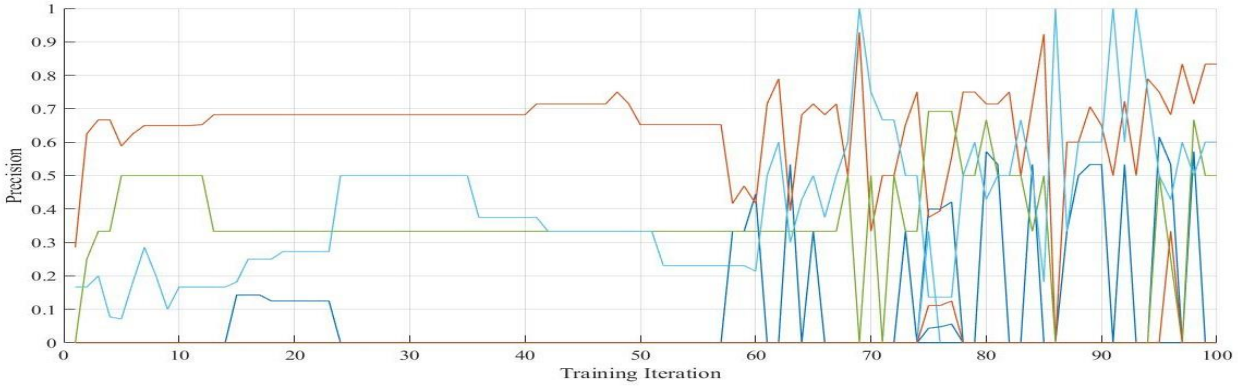

(c) Gaussian NN Precision

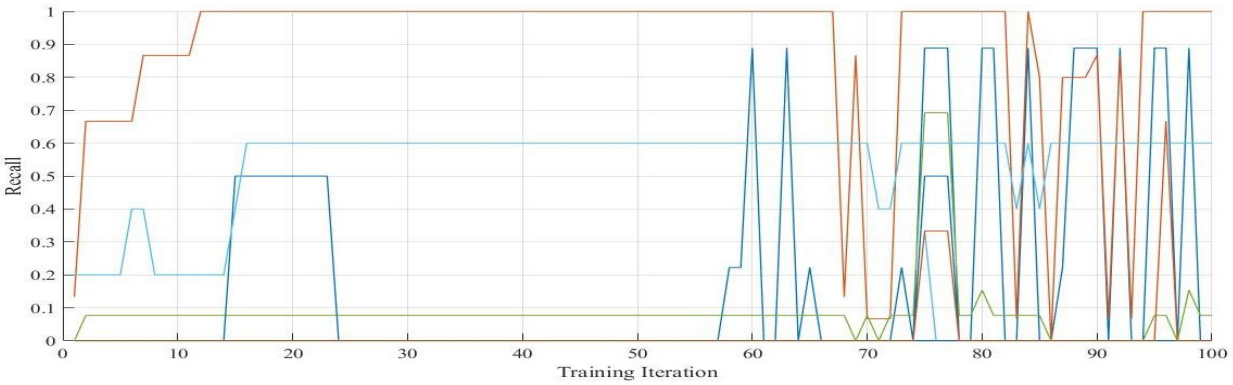

(d) Gaussian NN Recall/Sensitivity

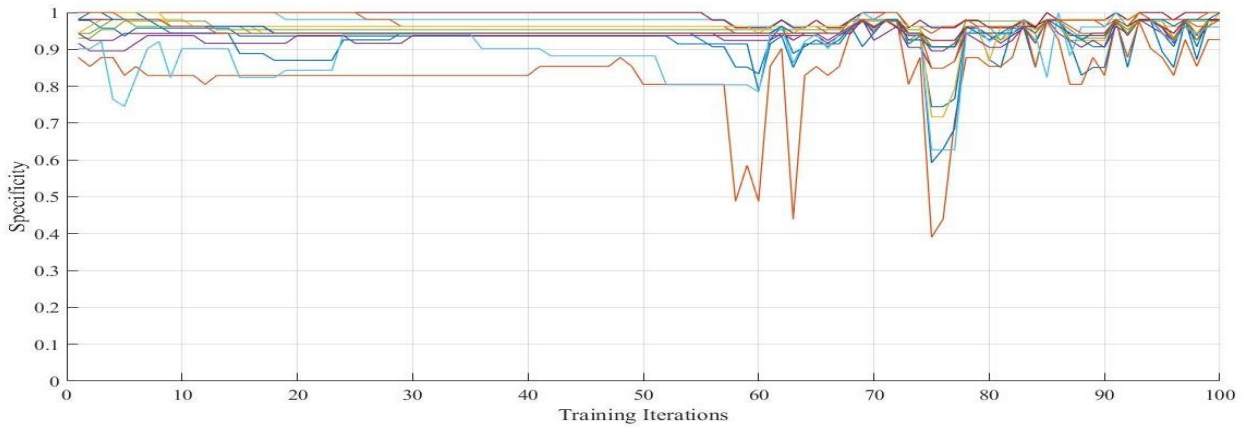

(e) Gaussian NN Specificity

Figure 29 – These graphs represent performance measures for Gaussian NN.

4 Conclusion

4.1 Discussions

For computerized identification of multiple retinal ailments from a publicly available STARE database, data was collected and separated into training and testing samples using biased random sampling by 70%, 30% split approach. Neural network approach when applied to the classification problem of retinal diseases revealed satisfactory results. Three activation functions Sigmoid, Gaussian and ArcTan performance was compared based on the training time of neural network and number of iterations performed across all performance measures i.e. accuracy, precision, specificity, F1 score and recall.

While collecting required data for our NN model, exclusion criteria was applied on images, diseases and features. After the <5 image criterion was applied, 19 diseases were selected from a total of 41 diseases, 37 features and 301 images from a total of approximately 400 images present in STARE database. When < 50 % occurrence criterion applied to 19 diseases, 37 features and 301 images, data was further reduced as 15 features and 112 were eliminated. Resulting valid images were 189, 22 features and same number of diseases i.e. 19 retinal diseases.

There were some images in the database that had only those features which were removed after exclusion criteria were applied hence those images also needed to be eliminated as those images were not satisfying < 5 image criteria hence, eliminated. Final selected data included 22 features, 16 retinal diseases and 186 valid images having both selected feature and disease information.

Firstly, Biased Random Sampling used to divide the selected data into training and testing samples. Biased random sampling was preferred over normal random sampling because:

- Total number of positive samples per disease vary from 5 to 51.
- With normal random sampling all positive samples of some diseases are selected for training, while down to 50% of the positive samples of some diseases are selected for training.
- Biasing the random sampling ensures the diseases with least number of positive samples are treated first while ensuring random sampling for training.

Secondly, a few of the diseases show good training and hence good detection, due to fair distribution of training examples. The neural network operates on some of the activation function, however discontinuous activation functions (e.g. ReLU) are trained and tuned within 2 or 3 iterations, however most of the diseases are overfit due to uneven data distribution. The continuous activation functions show a training trend which can be tracked. The Tan^{-1} activation function also faced overfitting of the data after 100 iterations. While sigmoid function fine tuned across all data and gaussian gave best performance.

< 5 image criteria can be changed and increased so that more data is gathered to achieve best results. In < 50 % occurrence criteria threshold value was set to 9 for 19 retinal diseases and the features with > 9 occurrence were eliminated. Threshold value can be increased as well to increase data for training samples.

4.2 Conclusions

This research concludes that multiple retinal diseases can be classified using computer aided machine learning methods. Gaussian function gave best performance within 500 iterations with 0.90 accuracy, 3.12 precision, 0.43 recall, 0.92 specificity and 0.11 F1 score at 500 iterations, but faced the problem of overfitting after 550 iterations. Sigmoid activation function was fine tuned across all iterations and did not go into data overfitting. ReLU and Tan^{-1} activation functions performed relatively poor as compared to sigmoid and gaussian.

4.3 Recommendations & Future Work

The best performance was obtained for the Gaussian Activation function with around 500 training iterations. For even better performance the number of features used can be increased from 22 and the data for diseases with very little positive samples can be modified. Another improvement can be to give weights to the training samples which are scarce for example retreat 3 positive training samples as 30 training samples, but this changes the data we are using

References

A. D., H., V., K., & Goldbaum, M. (2000). Locating blood vessels in retinal images by piecewise threshold probing of a matched filter response. *IEEE Transactions on Medical Imaging*, *19*(3), 203–210.

Abramoff, M. D., Garvin, M. K., & Sonka, M. (2010). Retinal Imaging and Image Analysis. *IEEE Reviews in Biomedical Engineering*, *3*, 169–208. https://doi.org/10.1109/RBME.2010.2084567

Aleynikov, S., & Micheli-Tzanakou, E. (1998). Classification of Retinal Damage by a Neural Network Based System. *Journal of Medical Systems*, *22*(3), 129–136. https://doi.org/10.1023/A:1022695215066

Alpaydin, E. (2004). *Introduction to Machine Learning* (First). Cambridge, Massachussetts: MIT Press. Retrieved from https://www.amazon.com/Introduction-Machine-Learning-1st-First/dp/B0086XGEVC

Aronow, W. S. (2012). Treatment of systemic hypertension. *American Journal of Cardiovascular Disease*, *2*(3), 160–170. Retrieved from http://www.ncbi.nlm.nih.gov/pubmed/22937486

Banerjee, S. (2006). A review of developments in the management of retinal diseases. *Journal of the Royal Society of Medicine*, *99*(3), 125–127. https://doi.org/10.1258/jrsm.99.3.125

Bjorn, V., Soutar, C., Irsch, K., Guyton, D. L., Burrows, A. M., Cohn, J. F., … Savvides, M. (2009). Anatomy of Eyes. In *Encyclopedia of Biometrics* (pp. 11–16). Boston, MA: Springer US. https://doi.org/10.1007/978-0-387-73003-5_253

Borkhade, G., & Raut, D. R. (2015). Support Vector Machine Neural Network Based Optimal Binary Classifier for Diabetic Retinopathy. Retrieved from https://www.semanticscholar.org/paper/Support-Vector-Machine-Neural-Network-Based-Optimal-Borkhade-Raut/32ddc6757672726f3808b4f5dbe404063bdbe01b

Boyd, S. R., Zachary, I., Chakravarthy, U., Allen, G. J., Wisdom, G. B., Cree, I. A., … Hykin, P. G. (2002). Correlation of increased vascular endothelial growth factor with neovascularization and permeability in ischemic central vein occlusion. *Archives of Ophthalmology (Chicago, Ill. : 1960)*, *120*(12), 1644–1650. Retrieved from http://www.ncbi.nlm.nih.gov/pubmed/12470137

Bradvica, M., Benašić, T., & Vinković, M. (2012). Retinal Vascular Occlusions. In S. Rumelt (Ed.), *Advances in Ophthalmology* (pp. 357–398). InTech. https://doi.org/10.5772/1258

Budai, A., Bock, R., Maier, A., Hornegger, J., & Michelson, G. (2013). Robust vessel segmentation in fundus images. *International Journal of Biomedical Imaging*, *2013*, 154860. https://doi.org/10.1155/2013/154860

Carmona, E. J., Rincón, M., García-Feijoó, J., & Martínez-de-la-Casa, J. M. (2008). Identification of the optic nerve head with genetic algorithms. *Artificial Intelligence in Medicine*, *43*(3), 243–259. https://doi.org/10.1016/j.artmed.2008.04.005

Chatterjee, S., Chattopadhya, S., Hope-Ross, M., Lip, P., & Chattopadhya, S. (2002). Hypertension and the eye: changing perspectives. *Journal of Human Hypertension*, *16*(10), 667–675. https://doi.org/10.1038/sj.jhh.1001472

Chen, Y.-H., Kuo, H.-K., & Kao, M.-L. (2003). Malignant hypertensive retinopathy-clinical and fundus manifestations in patients with new onset or acute exacerbation of chronic hypertension. *Chang Gung Medical Journal*, *26*(9), 669–677. Retrieved from http://www.ncbi.nlm.nih.gov/pubmed/14651165

Coleman, H. R., Chan, C.-C., Ferris, F. L., & Chew, E. Y. (2008). Age-related macular degeneration. *The Lancet*, *372*(9652), 1835–1845. https://doi.org/10.1016/S0140-6736(08)61759-6

Das, S., Dey, A., Pal, A., & Roy, N. (2015). Applications of Artificial Intelligence in Machine Learning: Review and Prospect. *International Journal of Computer Applications*, *115*(9), 31–41. https://doi.org/10.5120/20182-2402

Delacroix, S., Chokka, R. G., & Worthley, S. G. (2014). Hypertension: Pathophysiology and Treatment. *Journal of Neurology & Neurophysiology*, *05*(06). https://doi.org/10.4172/2155-9562.1000250

Dey, A. (2016). Machine Learning Algorithms: A Review. *International Journal of Computer Science and Information Technologies*, *7*(3), 1174–1179. Retrieved from www.ijcsit.com

Dharwal, R., & Kaur, L. (2016). Applications of Artificial Neural Networks: A Review. *Indian Journal of Science and Technology*, *9*(47). https://doi.org/10.17485/IJST/2016/V9I47/106807

Erden, S., Mefkure Ozkaya, H., Banu Denizeri, S., & Karabacak, E. (2016). The effects of home blood pressure monitoring on blood pressure control and treatment planning. *Postgraduate Medicine*, *128*(6), 584–590. https://doi.org/10.1080/00325481.2016.1189303

Esmaili, D. D., & Boyer, D. S. (2018). Recent advances in understanding and managing retinal vein occlusions. *F1000Research*, *7*, 467. https://doi.org/10.12688/f1000research.12886.1

Fasel, B. (2003). An introduction to bio-inspired artificial neural network architectures. *Acta Neurologica Belgica*, *103*(1), 6–12. Retrieved from http://www.ncbi.nlm.nih.gov/pubmed/12704977

Garner, A., & Ashton, N. (1979). Pathogenesis of hypertensive retinopathy: a review. *Journal of the Royal Society of Medicine*, *72*(5), 362–365. Retrieved from http://www.ncbi.nlm.nih.gov/pubmed/399635

Ghorbanian, S., Jaulim, A., & Chatziralli, I. P. (2012). Diagnosis and treatment of coats' disease: a review of the literature. *Ophthalmologica. Journal International d'ophtalmologie. International Journal of Ophthalmology. Zeitschrift Fur Augenheilkunde*, *227*(4), 175–182. https://doi.org/10.1159/000336906

Girish Jha. (2018). *Artificial Neural Networks and Its Applications*. Retrieved from https://www.researchgate.net/publication/228906616_Artificial_Neural_Networks_and_Its_Applications

Golan, S., Fisher, N., & Lowenstein, A. (2011). Current Treatment of Retinal Vein Occlusion. *European Ophthalmic Review*, *05*(01), 62. https://doi.org/10.17925/EOR.2011.05.01.62

Grosso, A., Veglio, F., Porta, M., Grignolo, F. M., & Wong, T. Y. (2005). Hypertensive retinopathy revisited: some answers, more questions. *The British Journal of Ophthalmology*, *89*(12), 1646–1654. https://doi.org/10.1136/bjo.2005.072546

Gulshan, V., Peng, L., Coram, M., Stumpe, M. C., Wu, D., Narayanaswamy, A., … Webster, D. R. (2016). Development and Validation of a Deep Learning Algorithm for Detection of Diabetic Retinopathy in Retinal Fundus Photographs. *JAMA*, *316*(22), 2402. https://doi.org/10.1001/jama.2016.17216

Gupta, M. P., Herzlich, A. A., Sauer, T., & Chan, C.-C. (2016). Retinal Anatomy and Pathology. In *Developments in ophthalmology* (Vol. 55, pp. 7–17).

https://doi.org/10.1159/000431128

Hamel, C. (2006). Retinitis pigmentosa. *Orphanet Journal of Rare Diseases*, *1*(1), 40. https://doi.org/10.1186/1750-1172-1-40

Han, J., & Moraga, C. (1995). The influence of the sigmoid function parameters on the speed of backpropagation learning (pp. 195–201). Springer, Berlin, Heidelberg. https://doi.org/10.1007/3-540-59497-3_175

Hayreh, S. S., Podhajsky, P. A., & Zimmerman, M. B. (2011). Natural History of Visual Outcome in Central Retinal Vein Occlusion. *Ophthalmology*, *118*(1), 119–133.e2. https://doi.org/10.1016/j.ophtha.2010.04.019

Hayreh, S. S., Zimmerman, M. B., Kimura, A., & Sanon, A. (2004). Central retinal artery occlusion. Retinal survival time. *Experimental Eye Research*, *78*(3), 723–736. Retrieved from http://www.ncbi.nlm.nih.gov/pubmed/15106952

Hildebrand, G. D., & Fielder, A. R. (2011). Anatomy and Physiology of the Retina. In *Pediatric Retina* (pp. 39–65). Berlin, Heidelberg: Springer Berlin Heidelberg. https://doi.org/10.1007/978-3-642-12041-1_2

Jaafar, H. F., Nandi, A. K., & Al-Nuaimy, W. (2010). Detection of exudates in retinal images using a pure splitting technique. In *2010 Annual International Conference of the IEEE Engineering in Medicine and Biology* (Vol. 2010, pp. 6745–6748). IEEE. https://doi.org/10.1109/IEMBS.2010.5626014

Jager, R. D., Mieler, W. F., & Miller, J. W. (2008). Age-Related Macular Degeneration. *New England Journal of Medicine*, *358*(24), 2606–2617. https://doi.org/10.1056/NEJMra0801537

Jain, N., & Juang, P. S. C. (2009). Retinal Artery Occlusion.

Kannabiran, C., & Mariappan, I. (2018). Therapeutic avenues for hereditary forms of retinal blindness. *Journal of Genetics*, *97*(1), 341–352. https://doi.org/10.1007/s12041-017-0880-x

Kauppi, T., Kalesnykiene, V., Kamarainen, J.-K., Lensu, L., Sorri, I., Raninen, A., … Pietila, J. (2007). the DIARETDB1 diabetic retinopathy database and evaluation protocol. In *Procedings of the British Machine Vision Conference 2007* (p. 15.1-15.10). British

Machine Vision Association. https://doi.org/10.5244/C.21.15

Kauppi, T., Kalesnykiene, V., Kamarainen, J., Lensu, L., Sorri, I., Uusitalo, H., … Pietila, J. (2006). DIARETDB0 : Evaluation Database and Methodology for Diabetic Retinopathy Algorithms. *Machine Vision and Pattern Recognition Research Group*, *1*, 1–17. https://doi.org/10.1093/icesjms/20.3.317

KEARNS, T. P., & HOLLENHORST, R. W. (1963). VENOUS-STASIS RETINOPATHY OF OCCLUSIVE DISEASE OF THE CAROTID ARTERY. *Proceedings of the Staff Meetings. Mayo Clinic*, *38*, 304–312. Retrieved from http://www.ncbi.nlm.nih.gov/pubmed/14043286

Konieczka, K., Flammer, A. J., Todorova, M., Meyer, P., & Flammer, J. (2012). Retinitis pigmentosa and ocular blood flow. *The EPMA Journal*, *3*(1), 17. https://doi.org/10.1186/1878-5085-3-17

Körner-Stiefbold, U. (2001). Central retinal artery occlusion (CRAO) – etiology, clinical signs and management. *Therapeutische Umschau*, *58*(1), 36–40. https://doi.org/10.1024/0040-5930.58.1.36

Kotsiantis, S. B. (2007). Machine learning: A review of classification and combining techniques. *Informatica*, *31*(3), 249–268. https://doi.org/10.1007/s10462-007-9052-3

Kumar Jaiswal, J., & Das, R. (2017). Application of artificial neural networks with backpropagation technique in the financial data. *IOP Conference Series: Materials Science and Engineering*, *263*(4), 042139. https://doi.org/10.1088/1757-899X/263/4/042139

Laouri, M., Chen, E., Looman, M., & Gallagher, M. (2011). The burden of disease of retinal vein occlusion: review of the literature. *Eye*, *25*(8), 981–988. https://doi.org/10.1038/eye.2011.92

Lim, L. S., Mitchell, P., Seddon, J. M., Holz, F. G., & Wong, T. Y. (2012). Age-related macular degeneration. *Lancet (London, England)*, *379*(9827), 1728–1738. https://doi.org/10.1016/S0140-6736(12)60282-7

Lin, M. K., Tsai, Y.-T., & Tsang, S. H. (2015). Emerging Treatments for Retinitis Pigmentosa: Genes and stem cells, as well as new electronic and medical therapies, are gaining ground. *Retinal Physician*, *12*, 52–70. Retrieved from

http://www.ncbi.nlm.nih.gov/pubmed/26503895

Ma, D. J., & Yu, H. G. (2016). Window to Heart; Ocular Manifestations of Hypertension. *Hanyang Medical Reviews*, *36*(3), 146. https://doi.org/10.7599/hmr.2016.36.3.146

Marcucci, R., Sofi, F., Grifoni, E., Sodi, A., & Prisco, D. (2011). Retinal vein occlusions: a review for the internist. *Internal and Emergency Medicine*, *6*(4), 307–314. https://doi.org/10.1007/s11739-010-0478-2

Mirshahi, A., Feltgen, N., Hansen, L. L., & Hattenbach, L.-O. (2008). Retinal vascular occlusions: an interdisciplinary challenge. *Deutsches Arzteblatt International*, *105*(26), 474–479. https://doi.org/10.3238/arztebl.2008.0474

Muhammad, I., & Yan, Z. (2015). SUPERVISED MACHINE LEARNING APPROACHES: A SURVEY. *ICTACT Journal on Soft Computing*, *05*(03), 946–952. https://doi.org/10.21917/ijsc.2015.0133

Natalie Schellack. (2015). Hypertension: A review of antihypertensive medication, past and present. *South African Pharmaceutical Journal*, *82*(2), 17–25. Retrieved from https://www.researchgate.net/publication/275030324_Hypertension_A_review_of_antihypertensive_medication_past_and_present

Noma, H., Funatsu, H., Mimura, T., & Hori, S. (2008). Changes of vascular endothelial growth factor after vitrectomy for macular edema secondary to retinal vein occlusion. *European Journal of Ophthalmology*, *18*(6), 1017–1019. Retrieved from http://www.ncbi.nlm.nih.gov/pubmed/18988180

Oetting Thomas & Jesse Vislisel. (2010). D Iabetic R Etinopathy :, (Frank 2004), 1–7.

Osareh, A., Mirmehdi, M., Thomas, B., & Markham, R. (2002). Comparative Exudate Classification Using Support Vector Machines and Neural Networks (pp. 413–420). Springer, Berlin, Heidelberg. https://doi.org/10.1007/3-540-45787-9_52

Patel, A., Nguyen, C., & Lu, S. (2016). Central Retinal Vein Occlusion: A Review of Current Evidence-based Treatment Options. *Middle East African Journal of Ophthalmology*, *23*(1), 44–48. https://doi.org/10.4103/0974-9233.173132

Pe'er, J., Folberg, R., Itin, A., Gnessin, H., Hemo, I., & Keshet, E. (1998). Vascular endothelial growth factor upregulation in human central retinal vein occlusion. *Ophthalmology*,

105(3), 412–416. https://doi.org/10.1016/S0161-6420(98)93020-2

Pei, Y. F., & Rhodin, J. A. G. (1970). The prenatal development of the mouse eye. *The Anatomical Record*, *168*(1), 105–125. https://doi.org/10.1002/ar.1091680109

Priya, R., & Aruna, C. P. (2012). SVM and Neural Network based Diagnosis of Diabetic Retinopathy. Retrieved from https://www.semanticscholar.org/paper/SVM-and-Neural-Network-based-Diagnosis-of-Diabetic-Priya-Aruna/78d6a826f49f65d715ef6533303b62adc83d7a1b

Rehak, J., & Rehak, M. (2008). Branch Retinal Vein Occlusion: Pathogenesis, Visual Prognosis, and Treatment Modalities. *Current Eye Research*, *33*(2), 111–131. https://doi.org/10.1080/02713680701851902

Ripley, B. D. (1996). *Pattern recognition and neural networks*. Cambridge University Press. Retrieved from http://www.stats.ox.ac.uk/~ripley/PRbook/

Rumelt, S., & Brown, G. C. (2004). A systematic approach to evaluate and treat retinal arterial occlusions. In *Handouts for a course on retinal arterial occlusions for the American Academy of ophthalmology Meetings*.

Sebastian, E. (2010). *The Complexity and Origins of the Human Eye: A Brief Study on the Anatomy, Physiology, and Origin of the Eye*. Liberty University. Retrieved from http://digitalcommons.liberty.edu/cgi/viewcontent.cgi?article=1123&context=honors

Shintani, K., Shechtman, D. L., & Gurwood, A. S. (2009). Review and update: Current treatment trends for patients with retinitis pigmentosa. *Optometry - Journal of the American Optometric Association*, *80*(7), 384–401. https://doi.org/10.1016/j.optm.2008.01.026

Sigler, E. J., Randolph, J. C., Calzada, J. I., Wilson, M. W., & Haik, B. G. (2014). Current management of Coats disease. *Survey of Ophthalmology*, *59*(1), 30–46. https://doi.org/10.1016/j.survophthal.2013.03.007

Sliney, D., & Wolbarsht, M. (1980). Review of Anatomy and Physiology of the Eye and Skin. In *Safety with Lasers and Other Optical Sources* (pp. 65–100). Boston, MA: Springer US. https://doi.org/10.1007/978-1-4899-3596-0_3

SPAIDE, R. F., LAUD, K., FINE, H. F., KLANCNIK, J. M., MEYERLE, C. B., YANNUZZI,

L. A., … COONEY, M. J. (2006). INTRAVITREAL BEVACIZUMAB TREATMENT OF CHOROIDAL NEOVASCULARIZATION SECONDARY TO AGE-RELATED MACULAR DEGENERATION. *Retina*, *26*(4), 383–390. https://doi.org/10.1097/01.iae.0000238561.99283.0e

Srinivasan, P. P., Kim, L. A., Mettu, P. S., Cousins, S. W., Comer, G. M., Izatt, J. A., & Farsiu, S. (2014). Fully automated detection of diabetic macular edema and dry age-related macular degeneration from optical coherence tomography images. *Biomedical Optics Express*, *5*(10), 3568–3577. https://doi.org/10.1364/BOE.5.003568

Staal, J., Abramoff, M. D., Niemeijer, M., Viergever, M. A., & van Ginneken, B. (2004). Ridge-Based Vessel Segmentation in Color Images of the Retina. *IEEE Transactions on Medical Imaging*, *23*(4), 501–509. https://doi.org/10.1109/TMI.2004.825627

Stahl, A., Agostini, H., Hansen, L. L., & Feltgen, N. (2007). Bevacizumab in retinal vein occlusion-results of a prospective case series. *Graefe's Archive for Clinical and Experimental Ophthalmology*, *245*(10), 1429–1436. https://doi.org/10.1007/s00417-007-0569-6

Visser, L. (2006). Common eye disorders in the elderly—a short review. *South African Family Practice*, *48*(7), 34–38. https://doi.org/10.1080/20786204.2006.10873425

Willoughby, C. E., Ponzin, D., Ferrari, S., Lobo, A., Landau, K., & Omidi, Y. (2010). Anatomy and physiology of the human eye: effects of mucopolysaccharidoses disease on structure and function - a review. *Clinical & Experimental Ophthalmology*, *38*, 2–11. https://doi.org/10.1111/j.1442-9071.2010.02363.x

Wong, T. Y., & McIntosh, R. (2005). Hypertensive retinopathy signs as risk indicators of cardiovascular morbidity and mortality. *British Medical Bulletin*, *73–74*(1), 57–70. https://doi.org/10.1093/bmb/ldh050

Wyszecki, G., & Stiles, W. S. (1982). *Color Science: Concepts and Methods, Quantitative Data and Formulae*. *Color Research & Application* (2nd ed.). New York: Wiley-Blackwell. https://doi.org/10.1002/col.5080080421

Zhu, J., Zhang, E., & Del Rio-Tsonis, K. (2012). Eye Anatomy. In *eLS*. Chichester, UK: John Wiley & Sons, Ltd. https://doi.org/10.1002/9780470015902.a0000108.pub2